Benjamin Pomes[1,2,3], Emmanuel Richaud[3] and Jean-François Nguyen[1,2,4]

[1]UFR d'Odontologie, Université Paris Diderot, Paris, France [2]Service d'Odontologie Groupe Hospitalier Pitié Salpêtrière, Paris, France [3]Arts et Metiers ParisTech, Laboratoire de Procédés et Ingénierie en Mécanique et Matériaux (PIMM), CNRS, CNAM, UMR 8006, Paris, France [4]PSL Research University, Chimie ParisTech CNRS, Institut de Recherche de Chimie Paris, Paris, France

7.1 MATERIAL SELECTION FOR MEDICAL APPLICATIONS: REQUIREMENTS FOR SEVERAL KINDS OF MEDICAL APPLICATIONS

A biomaterial is defined, according to the Consensus Conference of Chester (1992), as a material intended to interface with biological systems to evaluate, treat, increase, or replace any tissue, organ, or function of the body. According to the American National Institute of Health, a biomaterial is also described as "any substance or combination of substances, other than drugs, synthetic or natural in origin, which can be used for any period of time, which augments or replaces partially or totally any tissue, organ or function of the body, in order to maintain or improve the quality of life of the individual." Orthodontic brackets and surgical instruments are not included in this definition (Bergmann and Stumpf, 2013).

All materials used for replacing human tissues have joint specifications such as biocompatibility and they must also be noncytotoxic, nonallergic, nonimmunogenic, nonthrombogenic, and noncarcinogenic. Their specifications depend on their applications. Biomaterials suitable for dental restoration applications should meet these requirements:

- Nonirritating for the pulp and periodontal tissues.
- Low volumetric variation.
- Thermal insulation to protect the pulp from temperature variations.
- Esthetic and the stability of the different shades.
- Possible and simple repair and replacement.
- Easy handling.
- Resistance to water degradation and wear.
- Polishing ability to obtain a surface roughness limiting the adhesion of the plaque and thus to avoid secondary decay and periodontal diseases.

- Be compatible with sealing materials (bond, cement).
- Prevent leakage and saliva contamination and so dentinal hypersensitivity, coronary re-infection of the pulped tooth, secondary carious lesions and marginal dyschromias.
- Have mechanical properties adapted to the type of restoration and ideally the closest to the dental tissues:
  - Flexural strength greater than or equal to that of enamel ($\geq$380 MPa), and dentin (219 MPa).
  - Modulus of elasticity in the range of 90−98 GPa for enamel and 18−22 GPa for dentin.
  - Hardness Vickers in the range of $<$300 HVN for enamel.
  - Toughness in the range of 0.7−0.8 MPa $m^{1/2}$ for enamel, 2 MPa $m^{1/2}$ for dentin (Xu et al., 1998).

7.2 CHEMISTRY OF POLYMETHACRYLATES AND THEIR COMPOSITES

7.2.1 MONOMERS

7.2.1.1 Methyl methacrylate

Polymethyl methacrylate (PMMA) is the most well-known polymer of the methacrylate family, obtained from the in-chain polymerization of methyl methacrylate. It was developed in the 1930s by Hill and Crawford for Imperial Chemical Industries in England (Perspex), by Röhm and Haas in Germany (Plexiglas), and by Du Pont de Nemours in the United States (Lucite). It displays several interesting properties such as:

- A higher light transmission than glass (92% of visible light).
- A low density (1.18 g cm^{-3}) being about half that of glass.
- Shatter proof
- Softer and easier to scratch than glass (however, scratch-resistant coatings may be applied).

Its first applications as aircraft windows took place during World War II. Medical applications came later and include:

- In cardiology in pacemakers.
- For ophthalmology as artificial eye lenses for cataract surgery.
- For prosthetic dentistry in removable total and partial dentures (Fig. 7.1), temporary fixed denture, and restorative dentistry and for orthodontic devices.
- As bone cement for orthopedic surgery of the hip, knee, and other joints for the fixation of polymer or metallic prosthetic implants on living bone.

FIGURE 7.1

Removable total denture.

7.2.1.2 Other methacrylates for dental applications

In the 1950s, composite restorations were made from PMMA. Significant polymerization induced volume shrinkage and heat release as well as the release of methyl methacrylate monomers resulting in marginal discoloration, pulp reactions, and secondary caries. In 1956, Bowen tried to reduce shrinkage by using a bigger monomer: the bisphenol A surrounded by two glycidyl groups. However, moisture tended to inhibit polymerization. Bisphenol A glycidyl methacrylate (Bis-GMA, Fig. 7.2) was obtained by substituting end groups with methacrylate functions and offered an excellent solution to the problem (Bowen, 1962; Soderholm and Mariotti, 1999).

Bis-GMA has several advantages compared to PMMA, such as lower volatility, lower diffusion in dental tissues, and lower polymerization shrinkage because of its larger size, which explains its success. In addition, its tetrafunctional structure (i.e., two double bonds) makes it possible to obtain a crosslink network with better mechanical and physical properties.

However, Bis-GMA shows a high viscosity (1200 Pa s) (Barszczewska-Rybarek, 2009) because of its large size, and rigidity due to the two aromatic rings and especially its hydroxyl groups creating strong hydrogen intermolecular bonds between them which significantly reduces the mobility and make the molecule more hydrophilic. As it will be seen later, this involves a low conversion degree (DC)—39% in the case of photopolymerization and a limited incorporation of fillers as well as difficulty to handle the material (Sideridou et al., 2002).

Consequently, Bis-GMA is always associated with minor monomers such as triethylene glycol dimethacrylate—TEGDMA, with a viscosity of 0.011 Pa s

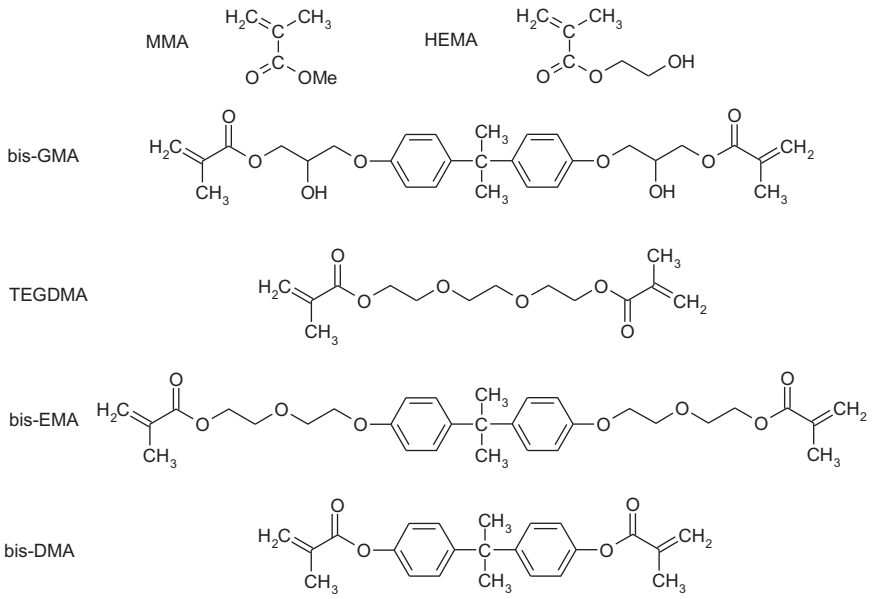

FIGURE 7.2

Some methacrylate monomers.

(Ilie and Hickel, 2011; Moszner and Salz, 2001)—or other derivatives such as bisphenol A ethoxyl dimethacrylate (Bis-EMA) (452 g mol^{-1}) and bisphenol A propoxyl dimethacrylate Bis-PMA (480 g mol^{-1}) and having a lower viscosity than Bis-GMA (because of its lower molar mass and the absence of hydroxyl groups).

UDMA monomers were developed in the 1970s by Forster and Walker (1974). Those UDMAs constitute a wide family of molecules differing by their molar mass and their structure (Fig. 7.3). The 1,6-bis(methacryloxy-2-ethoxycarbonylamino)-2,4,4-trimethylhexane is by far the most used and has a very low viscosity (23.1 Pa s) (Barszczewska-Rybarek, 2009).

7.2.1.3 Composition of the matrix

Monomers

Mixtures of several monomers are currently encountered in the literature for model and commercial materials. Usually, UDMA or Bis-GMA are used as major monomers together with minor monomers such as TEGDMA, HEMA, and bis-EMA for lowering the viscosity (Rüttermann et al., 2010; Rahim et al., 2012; Aljabo et al., 2015; Bhamra et al., 2010; Thomaidis et al., 2013). The use of minor monomers lowers viscosity which aims at incorporating more fillers to improve the mechanical properties, and to increase the conversion degree (Floyd and Dickens, 2006).

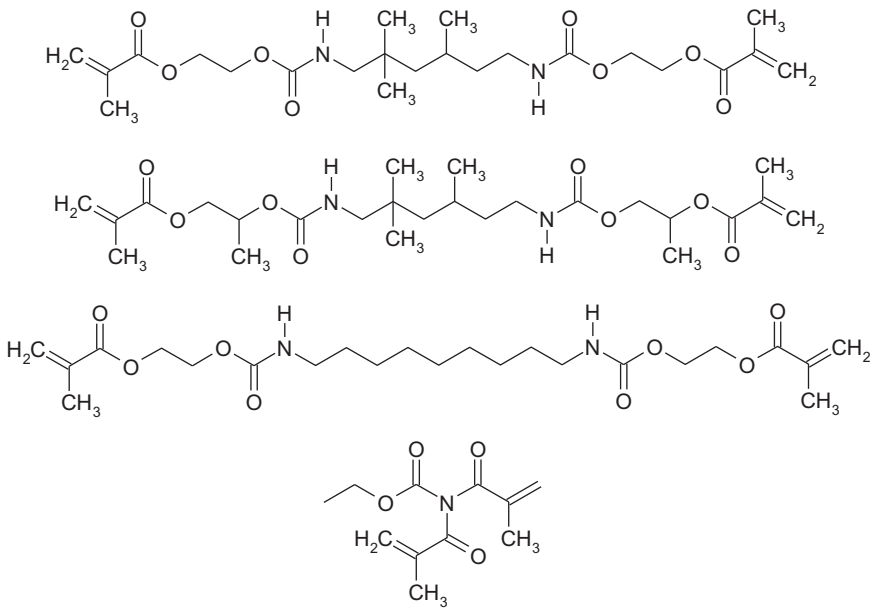

FIGURE 7.3

Some urethane dimethacrylate monomers.

Activators and polymerization initiators

The initiation of the polymerization reaction requires the creation of radicals coming from, for example:

- For chemopolymerization: amines (para-amino methyl acetate, para-toluenesulphonic acids, thioureas, and ascorbic acids) and peroxides (benzoyl peroxide as shown in Scheme 7.1, cumene peroxide, and terbutyl hydroperoxide).
- For photopolymerization: camphorquinone (Fig. 7.4) in combination with an aromatic amine. The camphorquinone displays an absorption in the range of 400−550 nm with a λ_{max} at 470 nm (Leprince et al., 2013) leading to radical generation, as illustrated in Scheme 7.2.

Polymerization inhibitors

Phenolic compounds react with free radicals and are used to avoid the possible spontaneous polymerization occurring during monomer storage.

Coupling agents

The coupling agent is an amphiphilic molecule bonding the hydrophilic inorganic filler and the hydrophobic resin. One of the most common molecules is 3-(Trimethoxysilyl)propyl methacrylate (Fig. 7.5).

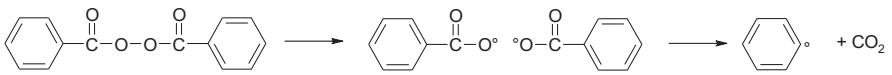

SCHEME 7.1

Initiation by benzoyl peroxide.

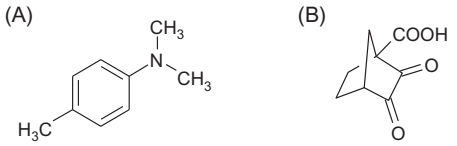

FIGURE 7.4

(A) 4,4 *N* trimethylaniline; and (B) camphorquinone used for initiating photopolymerization.

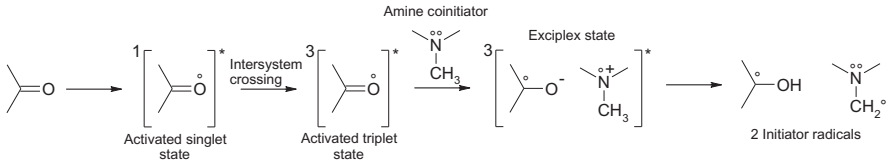

SCHEME 7.2

Activation of camphorquinone.

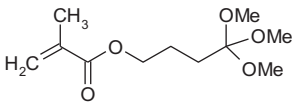

FIGURE 7.5

3-(Trimethoxysilyl)propyl methacrylate.

7.2.2 DENTAL COMPOSITES

Composite material can be defined as a combination of two or more immiscible materials of different chemical natures, leading to better properties than those of the individual components used alone. They are constituted by a matrix and dispersed reinforcements. In the case of an organic matrix, the reinforcement is an inorganic solid (glass, ceramic, metal) in the form of fibers, particles, or flakes. The properties of the composite material depend on the filler volume fraction, shape factor (or length:diameter ratio), and orientation (Kardos, 1993). The matrix allows the transmission of the mechanical stresses to the reinforcement, the

protection of this later against the external environment, and determines the conditions of use and processing.

Their composition has evolved since their introduction in odontology more than 50 years ago. Their clinical success would not have been possible without an understanding of the adhesion phenomena allowing their adhesion to dental tissues: enamel (Buonocore, 1955) and dentin (Nakabayashi et al., 1991).

The inorganic fillers may be silicas (SiO_2) in crystalline form such as quartz, or in amorphous form such as borosilicate glass, or heavy metal (Sn, Ba) glasses. Their shape can be angular (obtained by grinding), rounded (obtained by melting), or square with rounded corners (Raskin et al., 2006). Organomineral fillers are crushed prepolymerized composites and then added to the monomer/filler mixture, which makes it possible to reduce the shrinkage and to adapt the viscosity of the composite. Organoorganic fillers (trimethylolpropane trimethacrylate) and ceramics with grafted methacrylate groups (OrMoCers) (Raskin et al., 2006; Raskin, 2011) can also be used.

Composites can be classified according to the particle size and distribution of the fillers, the viscosity and the mode of polymerization, as dicussed next.

7.2.2.1 Particle size and distribution of fillers

Ferracane (2011) proposed to classify dental composites according to the fillers size (Fig. 7.6).

1. Macrofill: The first macrofill conventional composites presented 10−50 μm fillers, providing excellent mechanical properties, but difficulty in polishing and degradation at the surface by abrasion.
2. Microfill: microfill composites with 40−50 nm fillers were developed to overcome these disadvantages. They have good polishing properties, but low mechanical properties.
3. Hybrid: Hybrid composites are a mix of the particle sizes of the two previous families and, therefore, were used as a compromise between the mechanical, optical, and polishing properties.
4. Midfill: The tendency was then to reduce the size of the fillers to result in the hybrid midfill composites with charges of 1−10 μm and 40 nm.
5. Minifill: The evolution continued with the decrease in the size of the fillers with the minifill composites, with 0.6−1 μm and 40 nm filler, from which microhybrid composites were used for restorations in the anterior and posterior sectors.
6. Nanofill: The most recent innovations concern the development of nanofilled composites with 5−100 nm nanoparticules. However, this filler family has declined because of the difficulty of incorporating nanoparticles, the presence of numerous defects linked to the exponential increase of the matrix/fillers interface, and their high viscosity. To solve these problems, the nanofillers were partially sintered into nanoparticle aggregates (cluster) ranging from 5 to 75 nm in diameter (O'Brien, 2008).

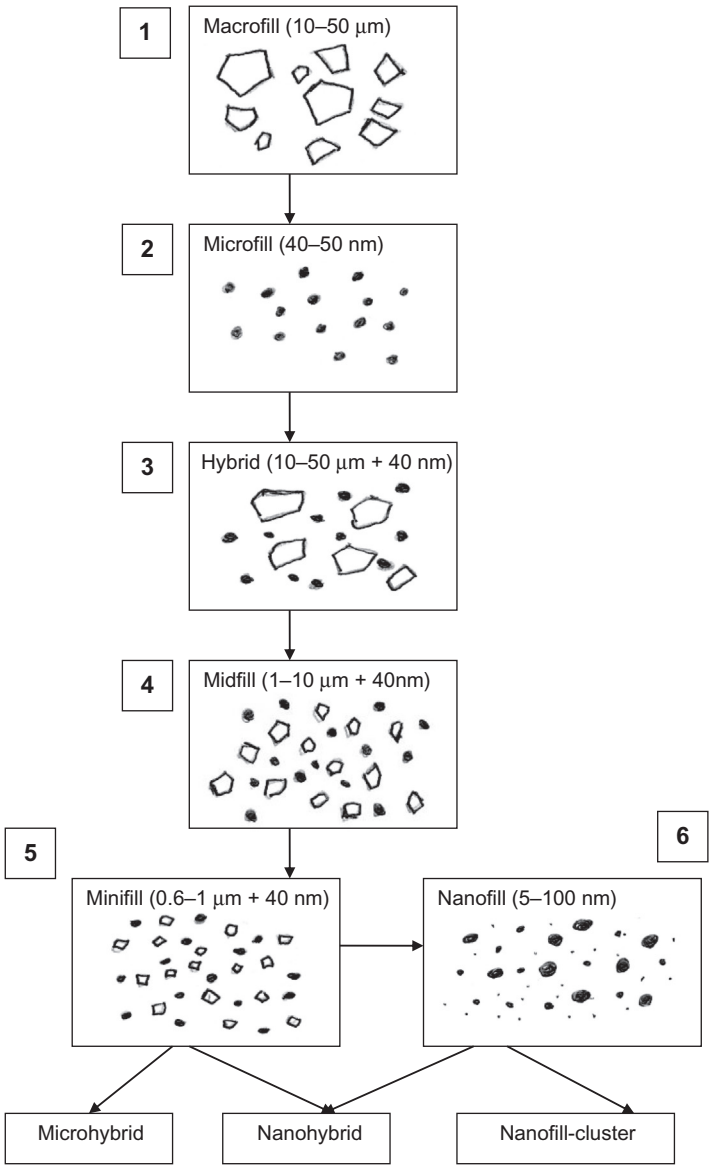

FIGURE 7.6

Classification of dental resin composites.

The size of filler particles incorporated into the resinous matrix of commercial dental composites tends to decrease over the years (Ilie and Hickel, 2011; Ferracane, 2011). Currently, microhybrid composites and nanohybrid composites (i.e., microhybrides with nanoparticles) are commercially available and display relatively close mechanical properties. Fiber-reinforced composites constitute a relatively new class of dental composites and are drawing increasing interest (Ballo and Närhi, 2017).

7.2.2.2 Viscosity

According to Einstein's formula, spherical fillers lead to a viscosity increase given by:

$$\eta = \eta_0 \cdot (1 + 2.5 \times \phi) \tag{7.1}$$

η and η_0 being, respectively, the viscosity of filled and unfilled resin, and ϕ the filler ratio (in volume). Adding c. 50%−60% fillers by weight (i.e., 80% in volume) leads to viscosity almost 30-times higher than for base resin (Papakonstantinou et al., 2013) and can reach more than 2000 Pa s.

Reactive mixtures for dental resin composites cover a wide range of viscosities which allow them to meet the requirements of numerous clinical indications. Fluid composites with low viscosity have 0.4−3 μm filler, a V_f of 42%−53%, are packaged as syringes (Fig. 7.7), and indicated for cervical restorations or for low-tissue losses. The high viscosity condensable composites have V_f of 66%−70% and are indicated for site tissue losses 1 and 2 (Sakagushi and Powers, 2012).

7.2.2.3 Polymerization mode

The composites can also be classified according to their mode of polymerization: photopolymerization (Fig. 7.8), chemopolymerization, dual photo- and chemopolymerization and more recently high-pressure high-temperature polymerization

FIGURE 7.7

Resin composite in syringe.

FIGURE 7.8

Polymerization lamp.

FIGURE 7.9

Polymer infiltrated ceramic network block suitable for CADCAM.

for industrial composite blocks suitable for CADCAM applications, which are discussed further next (Fig. 7.9).

Photopolymerization is usually performed using lamps with 150−600 mW cm^{-2} irradiance, for 10−60 seconds durations. Photopolymerization of dental resin composites is performed using LED or halogen light curing units with, respectively, an emission peak in the 450−470 nm (Issa et al., 2016) and 450−520 nm (Bala et al., 2005) wavelength ranges. The emission spectra and characteristics of some commercial lamps can be found in (Haenel et al., 2015).

CAD/CAM applications suitable for the manufacture of dental restorations are currently being developed (Van Noort, 2012; Miyazaki et al., 2009) because they obtain a constant quality. Chairside CAD/CAM can be used for prosthesis in dental surgery. In addition, blocks for CADCAM applications are manufactured industrially and so are more homogeneous and have fewer defects than handled materials.

Two types of blocks are currently commercially available: ceramic blocks and composite blocks. Ceramic blocks have superior mechanical properties and their chemical inertia which give them good biocompatibility. However, they are difficult to machine and cannot tolerate plastic deformations, which leads to the risk of fractures at the fine edges during the machining of the dental prosthesis. Thus, reoperation is more delicate. Composite blocks have lower mechanical properties, lower wear resistance and are less biocompatibile due to residual monomer release from incomplete polymerization. Nevertheless, they are easier to set on dental tissues and reoperation is easier. They also have better machinability and polishability. Indeed, the use of composite resin blocks designs for CAD/CAM significantly reduces the machining time and tool wear (Mainjot et al., 2016).

New technologies have been developed on polymerization and the methods for producing the blocks in order to increase the mechanical properties of the composites and to increase their strength, longevity, and biocompatibility.

Conventional thermopolymerization and photopolymerization have the disadvantage of being incomplete resulting in a low degree of conversion (56%−67%)

(Ferracane et al., 1997). Moreover, it induces internal stresses in the composite resulting from the shrinkage and the differential polymerization between the superficial part close to the source of irradiation and the deeper part (Ferracane, 2005).

To improve the mechanical properties of a composite, the polymerization mode can be enhanced. A previous study has shown that high temperature (180°C) and high pressure (250 MPa) polymerization allowed a significant increase in the mechanical properties of commercial composites compared to conventional photopolymerization (Nguyen et al., 2012).

Dispersed filler composite blocks are synthesized by thermopolymerizing (under high pressure or not) a mixture of mixed fillers and monomers (Mainjot et al., 2016; Nguyen et al., 2013).

PICN blocks present a particular microstructure as they are synthesized from a sintered glass-ceramic network with a ϕ_f greater than 73.8% in the form of a block, secondarily infiltrated by monomers, and then thermopolymerized under high pressure. Their fundamental characteristic is that they consist of two continuous networks imbricated in one another:

- A sintered glass-ceramic inorganic network with open porosity.
- An organic network constituted by the crosslinking of a dimethacrylic monomer inside the inorganic network.

The PICN microstructure allows for a higher fillers ratio compared to classical dispersion, and results in higher mechanical properties (Nguyen et al., 2013).

7.2.3 CHALLENGES IN IMPROVING PROPERTIES

Manufacturers try to improve dental composites performance by modifying the formulation of monomers and photoinitiators.

Composites with other monomers such as siloxane, oxirane, or silorane have been developed in order to attenuate the shrinkage, but do not provide significant improvement in the mechanical properties (Lien and Vandewalle, 2010).

Alternative photoinitiation systems based on mono-acyl phosphine oxide (MAPO), a bioacyl phosphorine oxide with a better production efficiency of free radicals than camphorquinone, allowing an increase in conversion degree, mechanical properties, and better polymerization in depth. These systems also improve biocompatibility because no tertiary amines are needed to generate free radicals. However, their absorption spectrum corresponds less to commercially available photopolymerization lamps (Leprince et al., 2013).

Improving composites is a complex process. Several papers have been aimed at comparing the performances of various reactive mixtures (Papakonstantinou et al., 2013; Fonseca et al., 2017). Indeed, changing the nature or ratio of a given component can induce undesired side effects (sometimes minor). The overall possible effects are summarized in Figs. 7.10−7.12.

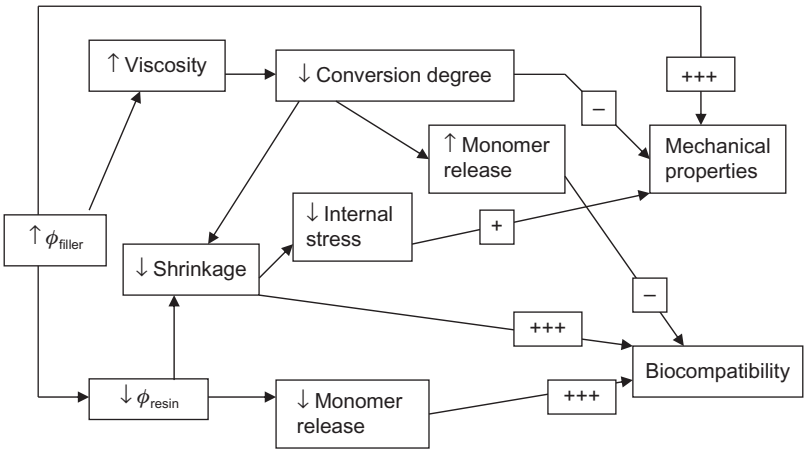

FIGURE 7.10

Effect of increasing the filler ratio (ϕ_f).

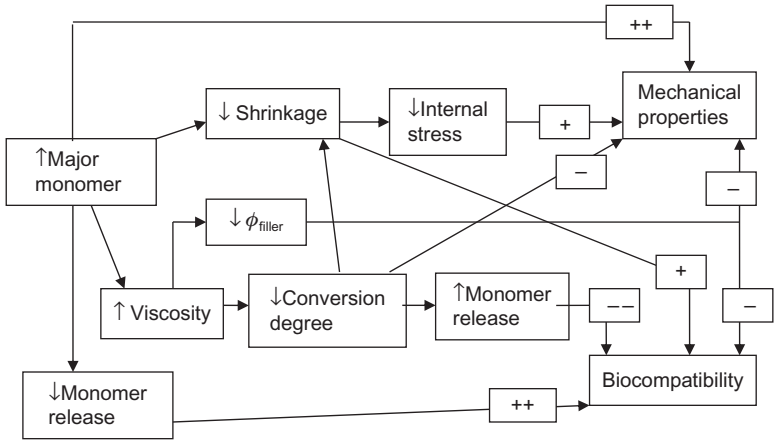

FIGURE 7.11

Effect increasing the concentration in the major monomer.

7.3 METHODS FOR MATERIAL SYNTHESIS

7.3.1 RADICAL POLYMERIZATION REACTION OF PMMA (DIFUNCTIONNAL MONOMER)

7.3.1.1 Mechanistic aspects

The anionic polymerization of MMA can be made in the presence of YCl_3/lithium amide of indoline/nBli (Ihara et al., 2007). Despite the interesting features of anionic MMA—polydispersity index close to 1, and possibility to get block

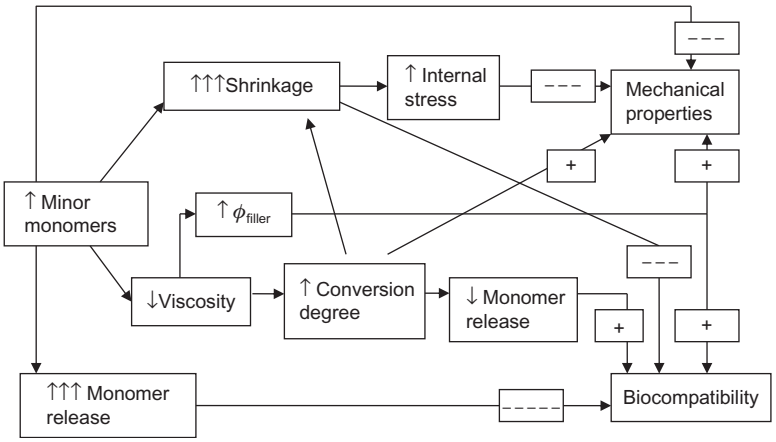

FIGURE 7.12

Effect increasing minor monomers.

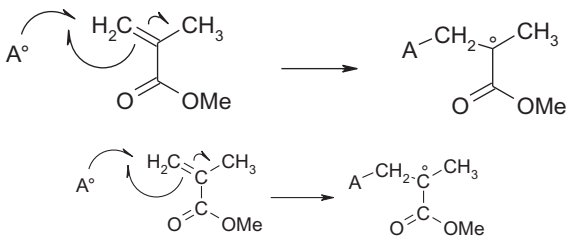

SCHEME 7.3

Chain initiation of MMA.

copolymers (Baskaran and Müller, 2007)—most of the industrial and medical PMMA grades are obtained from radical polymerization (O'Brien, 2008; Powers and Sakagushi, 2006).

The first step (initiation) corresponds to the creation of radicals by photo- or thermochemical processes (see Schemes 7.1 and 7.2, respectively):

$$A + \text{heat or UV} \rightarrow A^{\circ}$$

The free radicals break the C═C bonds of the monomers to form the first elements of the increasing polymer chain (Scheme 7.3). Then, during the propagation phase, polymers are formed by the successive addition of monomers (Scheme 7.4).

The propagation reaction which corresponds to the opening of C═C double bonds is, in essence, exothermic. The heat of polymerization is, thus, given by:

$$\Delta H_{\text{polym}} = \Delta H_{C=C} - \Delta H_{(\text{C}-\text{C})\text{monomer}} - \Delta H_{(\text{C}-\text{C})\text{monomer}-\text{monomer}} \qquad (7.2)$$

In PMMA, the hindering effect of acetyl groups make the third term quite low compared to other polymers so that the heat of polymerization is lower than for

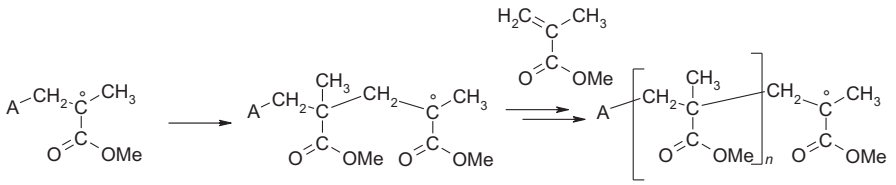

SCHEME 7.4

Chain propagation of PMMA.

other olefins (Roberts, 1950). However, the temperature in the bulk of a PMMA made bone cement polymerizing at room temperature reach about 80°C (Khandaker and Meng, 2015).

Finally, the termination phase closes the reaction by coupling two reactive polymers, or a reactive polymer with a reactive monomer, resulting in the formation of a stable covalent bond (Scheme 7.5).

One of the most remarkable properties of PMMA is that it is soluble in its monomer. In the applications of PMMA as bone cement, PMMA powder mixed with an initator (benzoil peroxide) is hence mixed with a MMA monomer containing *N,N* dimethyl *p*-toluidine (Asgharzadeh Shirazi et al., 2017). The PMMA is, hence, dissolved in monomer which polymerizes to give a glassy solid.

7.3.1.2 Kinetic aspects

The polymerization mechanism of MMA can be represented in a simple way as (Cardenas and O'Driscoll, 1976):

Initiation:	$I \rightarrow 2A^{\circ}$	k_d
	$A^{\circ} + M \rightarrow A\text{-}M^{\circ}$	k_i
Propagation:	$A\text{-}M_i\text{-}M^{\circ} + M \rightarrow A\text{-}M_{i+1}\text{-}M^{\circ}$	k_p
Termination:	$A\text{-}M_i\text{-}M^{\circ} + A\text{-}M_j\text{-}M^{\circ} \rightarrow A\text{-}M_{i+j+2}\text{-}A$	k_{t1}

It is assumed that the termination rate constants for combination and chain transfer to monomers are insignificant compared to the termination rate constant for disproportionation. Under the assumption of classical chemical kinetics (steady state hypothesis on A°, and on the overall concentration in radical species $[R^{\circ}]$), it can be shown that:

$$\frac{d[AM^{\circ}]}{dt} = 2k_d[A] - k_p[AM^{\circ}][M^{\circ}] - k_t[M]\cdot[R^{\circ}] \tag{7.3}$$

$$\frac{d[R^{\circ}]}{dt} = 2k_d[A] - k_t[R^{\circ}]^2 \tag{7.4}$$

$$r_{polymerization} = -\frac{d[M]}{dt} = \frac{2k_dk_p[A][M]}{k_t} \tag{7.5}$$

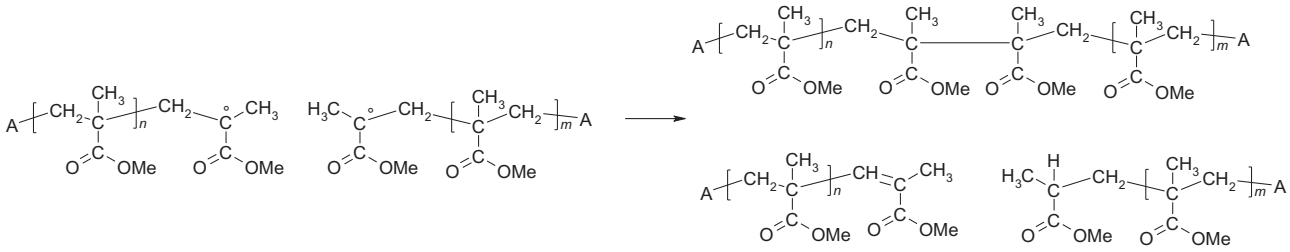

SCHEME 7.5

Chain termination of PMMA.

Table 7.1 Approximate Values of Kinetic Parameters for Polymerization (Initiation by AIBN)

k_d	s^{-1}	$10^{15}\cdot\exp(-61{,}000/RT)$
k_p	$l\ mol^{-1}\ s^{-1}$	$2.7\times10^{6}\cdot\exp(-10{,}600/RT)$
k_t	$l\ mol^{-1}\ s^{-1}$	$10^{8}\cdot\exp(-1400/RT)$

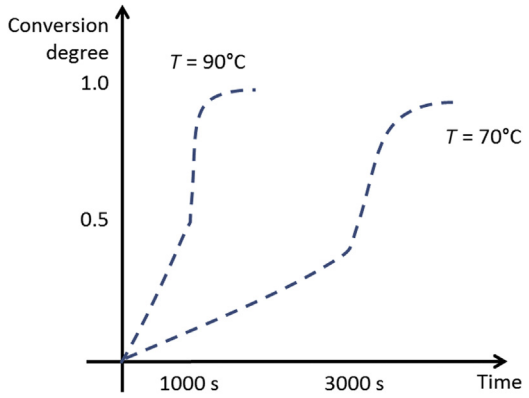

FIGURE 7.13

Monomer conversion versus polymerization time.

It can also be shown that the solution of those differential equations fairly represent the early stages of the polymerization reaction. Some values of kinetic parameters are given in Table 7.1 (Begum et al., 2012).

During polymerization, the molar mass increases, which lowers the mobility of radicals and the termination rate. At a certain stage, it results in observed autoacceleration (i.e., the "Thromsdorff effect"), as illustrated in Fig. 7.13. Cardenas and O'Driscoll (1976) proposed to model autoacceleration by using a termination rate constant for nonentangled growing chains and another for entangled ones. Later, Simon and colleagues (Begum and Simon, 2011) proposed a more-refined theory taking into account the role of free volume and its consequences on the diffusion rate of radicals. These developments, however, are out of the scope of this chapter.

The most interesting research deals with the copolymerization of several chemically different monomers which is relevant with reactive mixtures presented in Section 7.2.1.3. The theoretical treatment of copolymerization was proposed by Mayo and Lewis (1944). To summarize, the growing chain can be terminated either by an A or B site, which reacts either with a free A or B monomer:

---A° + A → ---AA°	k_{AA}
---A° + B → ---AB°	k_{AB}
---B° + A → ---BA°	k_{BA}
---B° + B → ---BB°	k_{BB}

The reactivity ratio k_{AA}/k_{AB} and k_{BA}/k_{BB} together with the composition of the reactive mixture, thus, give a prediction of the polymer composition and microstructure (i.e., random, alternating, or block copolymer). This theory was not, however, applied to methacrylates copolymers to the best of our knowledge.

7.3.2 POLYMERIZATION OF METHACRYLATE NETWORKS

7.3.2.1 Mechanistic aspects

Networks are used by using a tetrafunctional monomer (i.e., having two double bonds) such as dimethacrylates presented in Section 7.2.1.2. The processes is described in Scheme 7.6 for MMA:

This tetrafunctional behavior makes various kinds of intramolecular cyclization reactions possible together with intermolecular crosslinking as presented in Schemes 7.7 and 7.8 (Elliott et al., 2001).

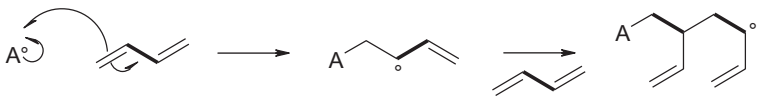

SCHEME 7.6

Initiation step for network polymerization.

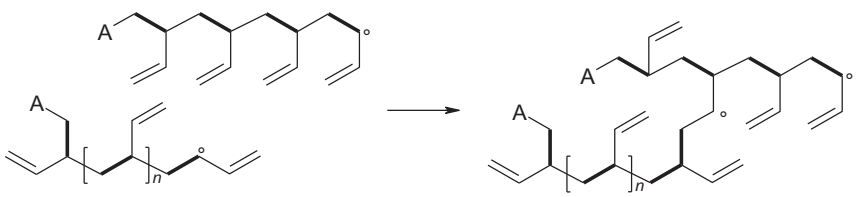

SCHEME 7.7

Mechanism of crosslinking.

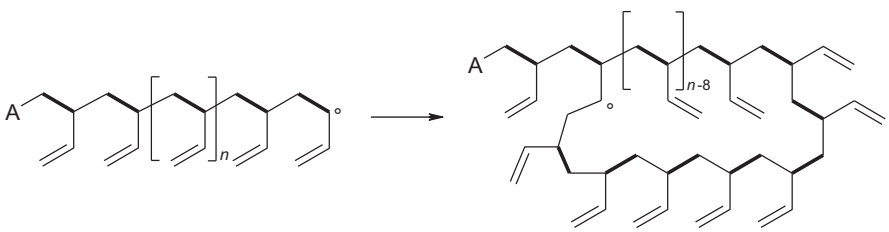

SCHEME 7.8

Mechanism of primary cyclization.

7.3.2.2 Polymerization kinetics

The polymerization of networks by radical polymerization is often divided into four successive steps as schematized in Fig. 7.14 (Pascault et al. 2002a).

The first step (pregel step) corresponds to the consumption of inhibitors and their reaction with monomers and the first propagations reaction.

The second step ("gel step") corresponds to the appearance of the first insoluble compounds. Growing chains react either with a monomer or by intramolecular primary cyclization. It results in the formation of crosslinked compact molecules very often called microgels, but better defined as crosslinked microparticles. The gel point is defined by a conversion degree at 1% in theory, but is observed in practice to be around 5% due to cyclizations. Despite the decrease in molecular mobility due to the continuous growth of polymer chains. Monomers can still diffuse and react at the periphery of the microgels in formation.

During the third step, the microgels connect to form macrogels which result in an increase in viscosity, so that the mobility of the polymers and monomers is reduced. At the end of this phase, the viscosity is so increased that termination reactions involving macromolecular radicals are inhibited, leading to a sudden autoacceleration of the polymerization rate.

The fourth step ("glassy step") corresponds to the vitrification where polymerization media turn to a glassy state, that is, that polymerization is frozen by lack of macromolecular mobility which explains why the conversion never reaches 100% (Dušek, 1996). The polymerization reaction can be completed only by an adequate postcuring step at temperatures higher than the glass transition of the vitrified network.

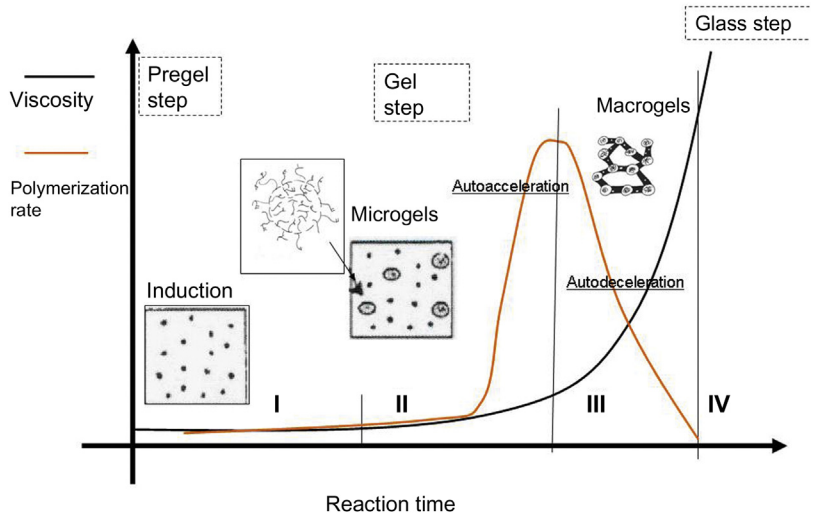

FIGURE 7.14

Kinetics aspects of network formation.

7.3.3 PARAMETERS INFLUENCING POLYMERIZATION

7.3.3.1 Intrinsic factors

Polymerization intrinsic factors depend essentially on the chemical composition and method of manufacture of the composite:

1. The viscosity of monomers is an important parameter for the polymerization kinetics and conversion of the dimethacrylate polymers by affecting the mobility and the reactivity of the monomers (Barszczewska-Rybarek, 2009).
2. Fillers decrease the conversion by increasing the overall viscosity of the composite and, locally, by reducing the mobility of the monomers around the fillers. For example, adding 50% fillers leads to a strong increase in viscosity (almost 30-times higher), but only a minor decrease in conversion degree (about 63% vs 61%) (Papakonstantinou et al., 2013). Furthermore, fillers can alter the photopolymerization by dispersing the photons superficially (Leprince et al., 2013).
3. Higher concentrations of initiator increases the conversion degree. Nevertheless, in the case of photopolymerization, when the initiator concentration exceeds an optimum value, the conversion degree decreases due to the excessive absorption of photons in the irradiated surface area and, thus, a decrease in the photon transmission in depth (Musanje et al., 2009).
4. Optical properties affect the photon transmission and, therefore, influence the conversion degree and the polymerization depth during photopolymerization. The photon transmission will be reduced in an opaque composite with a darker and more saturated hue, which increases the difference in degree of polymerization between the surface and at depth (Musanje and Darvell, 2006; Shortall et al., 1995). This is, for example, illustrated in (Aljabo et al., 2015) where 40%-filled composites displayed a conversion degree of about 70% at the surface versus c. 40% at a 4 mm depth.

7.3.3.2 Extrinsic factors

Temperature and pressure conditions influence polymerization. Higher temperature promotes molecular mobility. Higher pressure decreases molecular mobility (Murli and Song, 2010), but paradoxically has some beneficial effects on the reactivity (Schettino et al., 2008).

In the case of photopolymerization, the photon source affects the polymerization by its emission spectrum, irradiation time, irradiation distance, and polymerization protocol (Musanje et al., 2009). The effect of curing protocol on the main properties (glass transition, modulus, conversion degree) is developed in Dewaele et al. (2009).

7.3.4 POLYMERIZATION SHRINKAGE AND ITS CONSEQUENCES

The polymerization shrinkage of dental resins composite is inherent to polymerization reactions. This is due to the replacement of the Van der Waals bonds between

the monomers by covalent bonds and a decrease in the free volume (Kleverlaan and Feilzer, 2005). The shrinkage is about 1.5%−5% by volume (Floyd and Dickens, 2006; Ferracane, 2005) and depends on the concentration of the C═C of the monomers, the volume fraction of the composite, and the conversion degree.

The polymerization shrinkage is associated with stresses at the interface between the dental tissues and the composite restoration, and induces:

- Stresses on dental structures with fracture risks in enamel and dentine (Ferracane, 2005; Park and Ferracane, 2006).
- Stresses at the joint between the restorative material and the dental tissues resulting in leakage and postoperative sensitivities, marginal discolorations, bacterial contamination, and secondary caries.

This polymerization shrinkage also provokes contraction in the composite resin inducing internal stresses in the material (Ferracane, 2005).

7.4 PHYSICOCHEMICAL, BIOLOGICAL AND MECHANICAL PROPERTIES

7.4.1 STRUCTURE−PROPERTIES RELATIONSHIPS AND LINK WITH CLINICAL APPLICATIONS

7.4.1.1 Glass transition temperature and other transitions

The commonality of polymethacrylates obtained by radical polymerization is that they are amorphous materials. The main transition is the glass transition T_g separating the glassy and the rubbery regimes.

1. The glass transition of linear polymer (here PMMA) increases with molar mass, as described by the Fox-Flory's equation (Fox and Flory, 1950):

$$T_g = T_{g\infty} - \frac{K_{FF}}{M_n} \tag{7.6}$$

Some values of $T_{g\infty}$ and K are given for PMMA in Table 7.2.

Table 7.2 Flox-Flory Parameters for PMMA (Cardenas and O'Driscoll, 1976; Lu and Jiang, 1991)

	$T_{g\infty}$ (K)	K_{FF} (K kg mol^{-1})
a-PMMA	387	2.10^5
a-PMMA	388	21.10^4
i-PMMA	318	11.10^4
s-PMMA	405	20.10^4

2. The glass transition of thermoset networks increases with crosslinking density as, for example, illustrated in polymethylmecrylate networks crosslinked with ethylene glycol methacrylate (Gilormini et al., 2017) or other tetrafunctional acrylates (Loshaek, 1955).

The most general equation linking T_g increase with the conversion degree of monomer was proposed by Pascault and Di Benedetto (Pascault and Williams, 1990):

$$\frac{T_g - T_{g0}}{T_{g\infty} - T_{g0}} = \frac{\lambda x}{1 - (1 - \lambda)x} \tag{7.7}$$

where subscripts "0" and "∞" correspond to totally unreacted and totally reacted materials, λ is the ratio of heat capacity jump a T_g of cured and uncured materials $\Delta C_{p\infty}/\Delta C_{p0}$.

The glass transition of a fully cured network ($T_{g\infty}$) is given by DiMarzio's equation (DiMarzio, 1964):

$$T_{g\infty} = \frac{T_{gl}}{1 - (K_{DM} F n_0)} \tag{7.8}$$

where K_{DM} is the DiMarzio's constant equal to 2.91 for tridimensional networks such as epoxies (Bellenger et al., 1987), n_0 is the crosslink density (mol kg^{-1}) = $2/M_m$ if network is fully cured (M_m is the mass of monomer), T_{gl} is the glass transition of a "virtual" linear polymer ($n_0 = 0$), F is the flex parameter (kg mol^{-1}) related to the molar mass per rotatable bond.

The calculation of parameters of DiMarzio's law is illustrated in Bellenger et al. (1987) and Ernault et al. (2017). Some results are given in Table 7.3. In the case of UDMA, a good agreement is found with values obtained for materials being almost fully cured (Chi Phan et al., 2015).

However, Eqs. (7.7)−(7.8) show that T_g decreases dramatically if networks are not totally crosslinked, which is very often the case in networks cured at room temperature in dentistry. This is, for example, illustrated in the case of photocured Bis-GMA-TEGDMA (Table 7.4) (Stansbury, 2012).

The consequences of undercuring on mechanical properties at room temperature are illustrated, for example, by Ferracane et al. (1998). The main results are summarized in Table 7.5.

Table 7.3 Theoretical Maximum Glass Transition Temperature of Fully Cured Methacrylate Networks Used for Dental Applications

	T_{gl} (K)	F (g mol^{-1})	n_0 (mol g^{-1})	$T_{g\infty}$ (K)
BisGMA	327.4	18.3	0.0039	413.2
UDMA	320.6	15.4	0.00425	399
BisEMA	320.7	17.2	0.0037	394
TEGDMA	268.4	14.7	0.00699	382.9

Table 7.4 Characteristics of Photocured Bis-GMA-TEGDMA Networks

Curing time (s)	25	45	60	15
Conversion degree (%)	36.3	47.5	55.1	68.3
Approximative T_g (°C)	15	25	50	90

Table 7.5 Effect of Curing Degree in a Bis-GMA-TEGDMA (50/50) Matrix Reinforced with 62% Fillers

Conversion Degree (%)	E (GPa)	K_{IC} (MPa m$^{1/2}$)	σ_f (MPa)	Hardness (kg mm^{-2})
55	6.38	1.29	88.7	63.5
60	8.94	1.61	109.2	73.2
61	10.35	1.79	115.2	77.0
64	11.41	1.89	117.1	86.3
66	14.27	2.19	155.4	93.4

β transition corresponds to the activation of local mobility involving the group of atoms belonging to a monomer. It usually corresponds to a decrease in modulus: $\Delta E_\beta = 1300$ MPa. In the case of PMMA, a relative jump of 20% compared to "modulus at 0 K" (i.e., deduced from Eqs. 7.9−7.11) is reported (Gilbert et al., 1986). This transition is, however, not documented, to the best of our knowledge, for dental composites.

7.4.1.2 Short deformation properties

Typical stress−strain curves of PMMA at several temperatures and strain rates are schematized in Fig. 7.15 (Moy et al., 2011).

In dimethacrylate networks (Foroutan et al., 2011), stress−strain curves usually do not display any "hook" typical of a plastic deformation, which is why they are quite often characterized by their values of elastic modulus and ultimate strength.

The elastic behavior of a polymer originates from its cohesive energy which continuously decreases due to the thermal expansion increasing the interchain distance, and the activation of motions decreasing elastic modulus by ΔE_i at some given temperatures (e.g., β or γ transitions) (Gilbert et al., 1986):

$$E = E_0 \cdot \left(1 - \alpha \cdot \frac{T}{T_g}\right) - \sum \Delta E_i \tag{7.9}$$

According to the linear elasticity theory, Young's (E), bulk (K), and shear (G) modulus values at any temperature are interrelated by Eqs. (7.10)−(7.11):

$$E = 3 \cdot K \cdot (1 - 2v) \tag{7.10}$$

$$E = 2(1 + v) \cdot G \tag{7.11}$$

where v is the Poisson's ratio (see later).

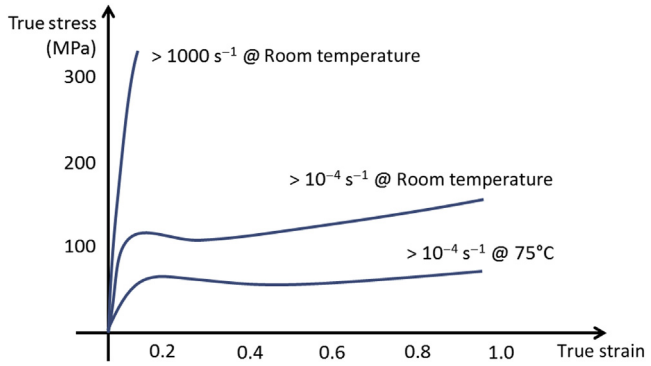

FIGURE 7.15

Typical stress–strain curves in PMMA.

Table 7.6 Estimation of Cohesive Energy and Compression Modulus

	E_{coh} (J mol^{-1})	V_m (cm^3 cm^{-1})	CED (MPa)	K (GPa)
TEGDMA	89,640	184.9	485	5.3
UDMA	169,530	342.9	494	5.4
Bis-GMA	225,930	339.4	666	7.3
Bis-EMA	185,930	393.4	473	5.2
PMMA	33,830	81.9	413	4.5

Their subglassy values K_0 and E_0 at very low temperature are shown to be correlated the cohesive energy density (CED) according to the formula (Pascault et al., 2002b):

$$K_0 \sim 11 \cdot \text{CED} \tag{7.12}$$

$$\text{CED} = \frac{E_{coh}}{V_m} \tag{7.13}$$

where E_{coh} is the cohesive energy (J mol^{-1}), V_m is the molar volume (cm^3 mol^{-1}), CED is the density of cohesive energy (MPa$^{1/2}$).

E_{coh} and V_m can be calculated according to the incremental method based on additive group's contribution proposed by Van Krevelen and Te Nijenhuis (2009), as shown in Table 7.6. If the Poisson's ratio is on the order of 0.3–0.4 (see later), the Young modulus of the matrix is, thus, expected to be close to 5 GPa.

However, experimental values are usually below these maximum values for several reasons, two of these being:

- Firstly, the undercured characteristics of the networks. A good example of modulus increase with conversion degree is given in Stansbury (2012) (see

also Table 7.5). The gelation is observed at a conversion degree about 7% at which materials are a visco-elastic solid having an elastic modulus c. 100 Pa. When the conversion degree reaches c. 20%, the modulus is close to 10 MPa. It exceeds 100 MPa when the conversion degree is more than 0.5.

- Secondly, the existence of several thermomechanical transitions increasing the mobility of groups, monomers, and later units made of several monomers (e.g., the β transition presented in Section 7.4.1.1 and decreasing, step-by-step, the modulus.

At room temperature, that is, presumably in the subglassy domain (between T_β and T_g), Young's modulus values are, thus, on the order of 1 GPa for some light-cured unfilled dimethacrylates (Sideridou et al., 2003; Bindu et al., 2013).

In the case of highly filled commercial materials, several equations describe the effect of fillers on mechanical properties (Atai et al., 2012). One of the most well-known is the Halpin-Tsai equation in the case of spherical fillers (Pal, 2005):

$$E_r = 1 + \frac{5}{2}\cdot\phi\cdot\left[\frac{2\left(\frac{E_d}{E_m}\right)-2}{2\left(\frac{E_d}{E_m}\right)+3}\right] \tag{7.14}$$

Despite the modulus of "pure" fully cured matrix is in the order of 5 GPa (see Table 7.7), it is not surprising that the elastic modulus of commercial dental materials increases linearly with filler content (see, e.g., Masouras et al., 2008) and can reach values c. 10 GPa (Ferracane et al., 1998; Papadogiannis et al., 2015; Jager et al., 2016b). It can be observed that the filler ratio influences the viscosity of the reactive mixture and later its conversion degree (see Fig. 7.10 and Ferracane et al., 1998) so that predicting the value of composites modulus remains intricate.

Experimentally, as illustrated in the case of PMMA (Mott et al., 2008), the modulus at very low temperatures can be estimated from ultrasonic measurements from a relationship between the longitudinal and the shear wave velocities (V_L and V_T) of the sample immersed in water and the density:

$$V_L = \sqrt{\frac{E_u}{\rho}\cdot\frac{1-\nu_u}{(1+\nu_u)(1-2\nu_u)}} \tag{7.15}$$

$$V_T = \sqrt{\frac{G_u}{\rho}} \tag{7.16}$$

Table 7.7 Poisson's Ratio of Polymethacrylates Used for Dental Applications

Resin	Filler		Poisson's Ratio
BisGMA + TEGDMA	40%	Colloidal silica 0.01–0.09 μm	0.372
BisGMA + TEGDMA	66%	Zircone + silica 0.01–3.5 μm	0.302
BisGMA + UDMA + BisEMA	60%	Zircone + silica 0.01–3.5 μm	0.308
BisGMA + TEGDMA	47%	Zircone + silica 0.01–6 μm	0.393

The Poisson's ratio (ν) in a composite can also be estimated from the volume fraction of fillers (ϕ), the Poisson's ratio of matrix, and filler ν_m and ν_f (Halpin and Kardos, 1976):

$$\nu = (1 - \phi)\cdot\nu_m + \phi\cdot\nu_f \tag{7.17}$$

Its value for matrices (0.3−0.35) increases at about 0.5 when T reaches T_g, that is, when the polymer turns from a glassy to rubbery state at which it is incompressible (Mott et al., 2008). In the case of filled dental composites (Chunga et al., 2004), values ranging from 0.3 to 0.4 are recorded at room temperature (Table 7.7).

Higher values are observed for commercial composites. According to several authors, hardness and elastic modulus are well-correlated (Thomaidis et al., 2013; Pal, 2005). Li et al. (2009a) propose, for example, a linear correlation:

$$E \sim 0.15 \times \text{Knoop Microhardness} \tag{7.18}$$

E being expressed here in GPa. The positive effect of curing on the microhardness is illustrated in Haenel et al. (2015) whereas Li et al (Atai et al., 2012) also show a decrease in hardness with polymer thickness.

Ultimate flexural strength has to display a value at least equal to 50 MPa for clinical requirements (as mentioned in Bindu et al., 2013). Typical values for dental composites are given in Table 7.8 (see Barszczewska-Rybarek, 2009).

According to Eyring's theory, plasticity originates in the jump of segments. This phenomenon is thermally activated (with a ΔH energy corresponding to the potential barrier) and facilitated by the activation volume v_{flow} and the external stress σ. The yield stress σ_Y is, thus, linked to the strain rate $\dot{\gamma}$:

$$\frac{\sigma_y}{2} = \frac{\Delta H}{v_{\text{flow}}} - \frac{kT}{v_{\text{flow}}}\cdot ln\left(\dot{\gamma}_0\dot{\gamma}\right) \tag{7.19}$$

This equation is close to the experimental observations by Kambour, according to which:

$$\sigma_Y = C\cdot\left(T_g - T\right) + \sigma_{Y0} \tag{7.20}$$

Table 7.8 Flexural Strength, Elastic Modulus, and Brinell Hardness for Some Unfilled Polymethacrylates Used for Dental Applications (Barszczewska-Rybarek, 2009)

Resin	σ_f (MPa)	E (MPa)	HB (N mm^{-2})
Poly(bis GMA)	115	3800	75
Poly(TEGDMA)	85	3900	135
Poly(UDMA)	140	3500	165
Poly(bisGMA-*co*-TEGDMA)	95	4100	90
Poly(bisGMA-*co*-TEGDMA-*co*-UDMA)	105	2800	190

C ranges from 0.5 to 1 MPa K^{-1} (Cooke et al., 1998; Li and Strachan, 2011). A decrease in glass transition, thus, results in a decrease in yield stress.

At temperatures above the glass transition, thermoset networks are in a rubbery state. Elastic behavior is given by the Flory approach according to which the Young's modulus is proportional to the concentration in elastically active chains n_0 (Mark, 1984):

$$E = \frac{3\rho RT}{M_C} = 3 \cdot n_0 RT \tag{7.21}$$

where ρ is the density, M_C the average molar mass between crosslinks, R the gas constant, and T the absolute temperature. Values of rubbery modulus (measured at 175°C) of several bis-GMA + HEMA networks close to 25 MPa are given in Park et al. (2009). This means that the average molar mass between crosslink nodes is c. 400−500 g mol^{-1} (i.e., n_0 c. 2 mol kg^{-1}). This is the expected order of magnitude in these materials (see Table 7.3) since the HEMA comonomer contributes to an increase of the molar mass between crosslinks.

The correlation between rubbery modulus and conversion degree is illustrated in the case UDMA by Sadoun and colleagues (Chi Phan et al., 2015). Identically to glassy modulus, it increases with filler content (Munhoz et al., 2017) as described by Guth (1945):

$$E = E_0.(1 + 2.5\phi + 14.1\phi^2) \tag{7.22}$$

where $14.1 \times \phi^2$ expresses the filler−filler interaction effect on elasticity and is particularly relevant for highly filled matrices such as dental composites.

Even if Young's modulus on the rubbery plateau is not itself helpful data for practitioners, it is noteworthy that it allows an estimation of the concentration in elastically active chains, expected to decrease during hydrolytic degradation (see Section 7.5.3).

7.4.1.3 Ultimate properties

The toughness expresses the ability of a material to absorb energy and plastically deform without fracturing. According to the Griffith's equation, the stress intensity factor in an infinite plate with a crack of $2a$ length is:

$$K_I = y \cdot \sigma \cdot (a.\pi)^{1/2} \tag{7.23}$$

that is, that sample fails either if the stress σ, or the size of the crack a, exceed a critical value.

PMMA toughness can be easily studied using a common tensile test sample. In the case of dental composites, various methods are proposed, for example, using notched disks (Watanabe et al., 2008) allowing to study failure in mode I or II. The values of toughness are shown to depend on the load rate, but stay close to 1.5 MPa $m^{1/2}$ (Wada, 1992). These values are actually very close to unreinforced poly(UDMA) (Phan et al., 2014) and, more unexpectedly, in filler reinforced composites (Atai et al., 2012; Guth, 1945; Ornaghi et al., 2014).

Reversely, the toughness can reach about 2.5 MPa $m^{1/2}$ for resins reinforced with 7.5% short glass fibers (Bocalon et al., 2016). The presence of rubbery fillers has a positive effect on toughness (Mante et al., 2010; Omran Alhareb et al., 2017).

The impact strength is typically measured using a Charpy impact test on notched or unnotched samples. The typical value for PMMA is about 5 kJ m^{-2} with possible improvements by reinforcing with various kinds of rubbery particles (NBR (Omran Alhareb et al., 2017) or poly(methyl methacrylate-b-butyl acrylate-b-methyl methacrylate) (MAM) (Lalande et al., 2006). In unfilled poly(UDMA), poly(Bis-GMA), poly(TEGDMA), and their mixtures the value is higher and can reach c. 9 kJ m^{-2} (Barszczewska-Rybarek, 2009).

Lastly, it is noteworthy that the combined effect of fillers and low monomer viscosity lead to porosities (Balthazard et al., 2014) which are quite detrimental to the ultimate mechanical properties. It must also be highlighted that the difference between the thermal coefficient dilatation of the polymer filler induces stresses at the polymer/filler interface (Ferracane, 2005) which becomes an area of weakness where a crack will easily propagate and reduces the toughness of the material.

7.4.2 BIOCOMPATIBILITY

The biocompatibility of dental resins may affect both the patient and the dentist.

In the case of samples immersed in water, it can be observed that a part of the mass is lost presumably because of the migration of low molecular mass compounds (Sideridou and Karabela, 2011).

Those phenomena are usually quantified by measuring the soluble fraction, being the relative mass decrease of a composite resin before immersion and after immersion and complete drying. If the results clearly depend on the curing process, it seems that this soluble part can represent from 0.1% to 1% by weight of the polymer mass in common light-cured dimethacrylate matrices (Rüttermann et al., 2010; Sideridou et al., 2003). This quantity can even be higher if low molecular mass compounds produced from the partial hydrolytic or enzymatic degradation of networks, which will be addressed in the following of this chapter.

As expected with uncompletely cured networks, a great part of soluble (eluted from resins) compounds contains unreacted monomers and photoinitiators (Munhoz et al., 2017; Ferracane, 2006). The migration of a chemical out of a polymer is, in great part, controlled by its molar mass (expressing the architecture) of compounds so that it is quite likely that dimers or trimers diffusion is slow enough to be neglected in the first approach.

Quite interestingly, it was observed that the fraction of UDMA and Bis-GMA extracted from UDMA-TEGDMA or Bis-GMA/TEGDMA was systematically higher than their fraction in the polymerization mixture. Since their higher molar mass makes them less mobile than TEGDMA monomers, this suggests that Bis-GMA and UDMA are not randomly polymerized with TEGDMA (Floyd and Dickens, 2006) (see Section 7.3.1.2).

The toxicity of several kinds of chemicals involved in the formation of dental composites was addressed by Thonemann et al. (2002). According to TC50 measurements performed on several kinds of cells, Bis-GMA seems by far to display the highest cytotoxicity compared to UDMA and MMA.

Wear debris are produced from attrition and abrasion of resin composite dental restorations (Heintze, 2006). Ingestion of filler particles could result in potential harm to the liver, kidney, or intestine (Gatti and Rivasi, 2002; Gatti, 2004). Nevertheless there is no scientific evidence that swallowed particles induce a significant health risk for patients (Heintze, 2006).

Besides this, polishing, shaping, and grinding composites result in particle dust ($<5\,\mu m$ particles including nanoparticles <100 nm) which can be inhaled and penetrate the lungs (Van Landuyt et al., 2012), provoking cell toxicity in human bronchial epithelial cells (Cokic et al., 2016)—for exposure under relatively high particle concentrations compared to standard use.

The fiber-reinforced composites were recently introduced and seem to offer a good combination of reinforcement of mechanical properties and low toxicity (Ballo and Närhi, 2017).

7.5 LONG-TERM BEHAVIOR

Let us recall that there are two kinds of ageing phenomena:

- Physical ageing, where the polymer backbone remains unmodified, whereas the free volume is changed by physical relaxation, the ingress of an external penetrant, or the loss of an adjuvant (typically a plasticizer).
- Chemical ageing where the polymer backbone or its lateral groups undergo chain scissions or crosslinking induced by any kind of chemical reaction.

In the specific case of polymeric dental materials, the main mechanisms were listed by Ferracane (2006). The most relevant ones for acrylates will be addressed next.

7.5.1 AGING BY PHYSICAL RELAXATION

This kind of mechanism is common to every glassy polymer. When cooled from elevated temperatures, the specific volume decreases, but the decrease rate is below the T_g of the polymer. Lower than this temperature, the polymer can be considered as in an "out-of-equilibrium" state. The primary thermodynamic properties (volume, enthalpy, etc.) decreases slowly during the storage at an ageing temperature (T_a) lower than T_g (Fig. 7.16).

Meanwhile, the necessary enthalpy for initiating rubbery phase motions is increased when reheating above T_g, generating the enthalpy overshoot commonly

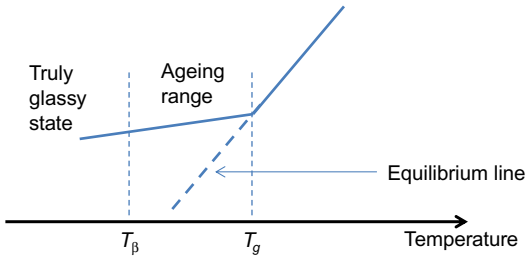

FIGURE 7.16

Mechanism of physical relaxation ageing. T_g is the glass transition temperature, T_β the highest temperature of subglassy transition, and v is the specific volume (Struik, 1978).

observed by DSC (Diaz-Calleja et al., 1987) and a slight increase of T_g toward a "fictive temperature" (T_f) given by:

$$T_f = T_g - \frac{\Delta h}{\Delta c_P} \tag{7.24}$$

The enthalpy overshoot tends toward an asymptotical value given by:

$$\Delta h_\infty = \Delta c_P \cdot (T_g - T_a) \tag{7.25}$$

where $\Delta c_P = c_{Pl} - c_{Pg}$ is the heat capacity jump at T_g, and T_a is the temperature at which physical ageing occurs.

From a practical point of view, the distance to equilibrium increases with decreasing temperature, but the rate decreases very strongly when temperature decreases, so that this ageing mechanism is typically significant in the temperature range [T_g; $T_g - 60°C$] (Pethrick and Davis, 1998).

Physical ageing is described by a distribution of relaxation times:

$$\phi(t) = \exp\left[-\left(\frac{t}{\tau}\right)^{\beta}\right] \tag{7.26}$$

The function seems to depend on the experimental technique (e.g., dynamic modulus, dilatometry, calorimetry) used for measuring (Pérez et al., 1991).

τ is the relaxation time that can be predicted by two models (Hodge, 1994):

1. Tool–Narayanaswamy–Moynihan model predicts the relaxation time from the value of "fictive" temperature (Narayanaswamy, 1971):

$$\tau = \tau_0 \cdot exp\left[\frac{x\Delta h^*}{RT} + \frac{(1-x)\Delta h^*}{R.T_f}\right] \tag{7.27}$$

2. Kovacs–Aklonis–Hutchinson–Ramos (KAHR) (Grassia and Simon, 2012; Grassia and D'Amore, 2011):

$$\tau = \tau_R \cdot \exp[\theta \cdot (T_R - T)] \cdot exp\left[-(1-x) \cdot \frac{\theta \cdot \delta}{\Delta \eta}\right] \tag{7.28}$$

where τ_R is the relaxation time at the reference temperature T_R, θ is linked to activation energy, x is an adjustable parameter ranging from 0 to 1, η is parameter specific to the value under study (i.e., depending on heat capacity [c_P] for enthalpic relaxation, dilatation coefficient α for volumetric relaxation).

The full description of these models is out of the scope of this chapter.

Since ageing by physical relaxation results in a decrease of free volume quantity, all physical and mechanical properties related to free volume are changed, for example:

- Yield stress is increased, possibly because the activation volume v_{flow} (see Eyring's equation) is linked to the residual free volume.
- Creep resistance (Hutchinson and Bucknall, 1980)
- Toughness (Arnold, 1995),
- Loss tangent is decreased in the domain of the subglassy transition (c. 320K in the case of PMMA) (Diaz-Calleja et al., 1987; Etienne et al., 2007) (see Fig. 7.17).

A final consequence is worth being investigated. It seems clear that physical ageing relaxation induces free volume collapse, i.e., a decrease in the size of nanovoids present in the polymer (Pethrick and Davis, 1998) with possible consequences on the water ingress in the composite.

7.5.2 HUMID AGEING

The penetration of water is an environmental factor that can drastically limit the performance of polymers. Two subcases can be distinguished:

- Water diffuses into the polymer, but does not change the polymer's architecture.
- Water diffuses and reacts with the polymer, generating scission of lateral or skeletal bonds (Section 7.5.3).

7.5.2.1 *Water solubility*

The mechanism of the polymer−water interaction can be, firstly, described by the shape of the sorption isotherm where the ratio of water in the polymer−water mixture is plotted by the function of water activity (or partial pressure), as illustrated in Fig. 7.18.

Several shapes of sorption isotherms are described for the sorption of gases into polymers. In the case of water penetration, three main cases exist:

1. Henry's law is the simplest theory for water dissolution. It is associated to a very dilute solution behavior in which dissolved water molecules are few and far between. It assumes that maximum (equilibrium) water uptake is directly proportional to the external water partial pressure:

$$C = s \cdot P \tag{7.29}$$

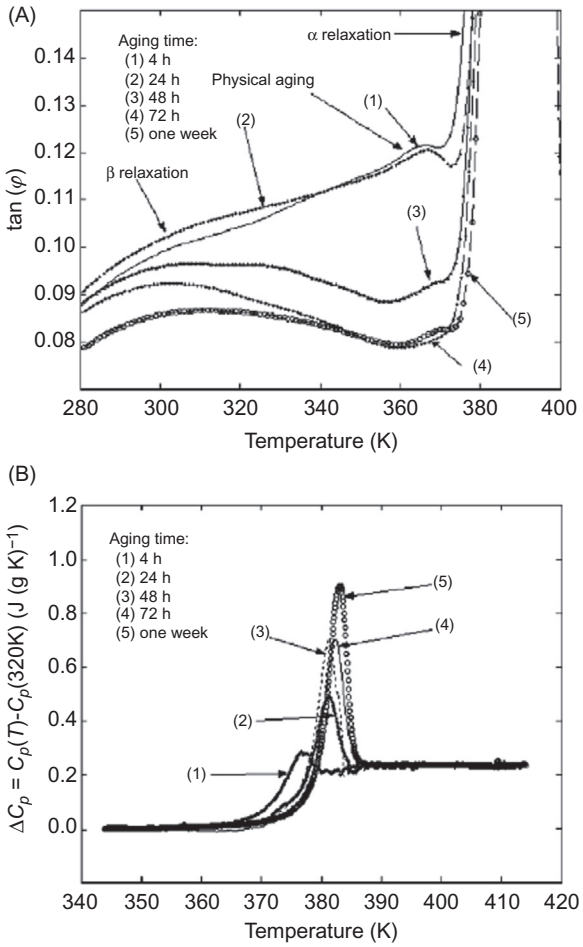

FIGURE 7.17

The effect of physical ageing on PMMA at 363 K after thermal annealing on: (A) loss factor; and (B) specific heat.

Reused with permission of Elsevier.

where C is solubility expressed, for example, in cc(STP)/cc(polymer).

s is the solubility coefficient (expressed in mol L^{-1} Pa^{-1}) expected to obey Van't Hoff law:

$$s(T) = s_0 \cdot exp\left(-\frac{\Delta H_S}{RT}\right) \tag{7.30}$$

P is the water partial pressure (expressed in Pa) obeying Clapeyron's law:

$$P(T) = P_0 \cdot \exp\left(-\frac{\Delta H_{vap}}{RT}\right) \tag{7.31}$$

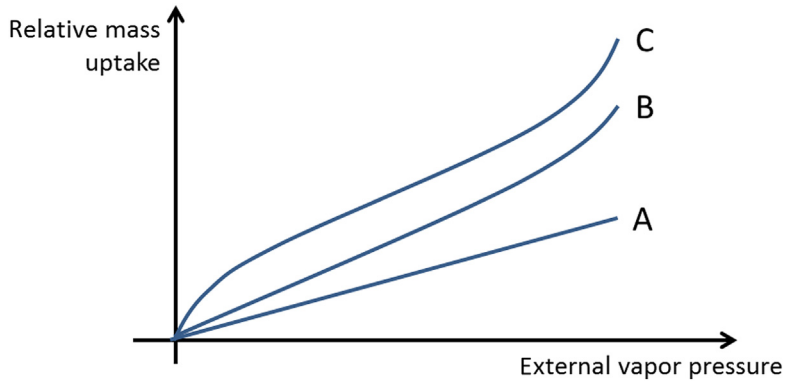

FIGURE 7.18

Shape of sorption isotherms in polymers.

The apparent activation energy for water equilibrium concentration is, thus, given by:

$$E_S = -\Delta H_S - \Delta H_{\text{vap}} \tag{7.32}$$

ΔH_{vap} is close to 43 kJ mol^{-1}.

In PMMA, $\Delta H_S \sim -43$ kJ mol^{-1} so that water uptake does not depend on temperature as in the first approach (Barrie and Machin, 1971).

2. An isotherm which is linear at low activity and displays an upturn at higher water pressures (such as B isotherm in Fig. 7.18) is associated to a type III isotherm in the BET classification and is sometimes called a Flory Huggins isotherm. This upturn has two explanations:

a. Due to clustering of solvent molecules.

b. Due to plasticization of the polymer matrix induced by solvent sorption.

The mathematical description of Flory Huggins isotherms is given by:

$$\ln P/P_0 = \ln(1-\phi_p) + \phi_p + \chi\phi_p^2 \tag{7.33}$$

where ϕ_p is the volume fraction of the polymer in the water–polymer mixture. is the Flory parameter describing the polymer–water affinity, expressed by:

$$\chi = \frac{V_{mwater}}{RT}\cdot\left(\delta_{polymer} - \delta_{water}\right)^2 \tag{7.34}$$

where V_{mwater} is the molar volume of water, $\delta_{polymer}$, and δ_{water} are, respectively, the solubility parameters of polymer and water, R the ideal gas constant and T the absolute temperature.

In the case of PMMA-water association, both solubility parameters are known: $\delta_{\text{PMMA}} = 19.0$ MPa$^{1/2}$ and $\delta_{water} = 47.9$ MPa$^{1/2}$. However, the resulting χ parameter seems to be an overestimation (5.91 at 35°C) compared to the value deduced from sorption isotherms (3.48). One possible explanation

is that this estimation of χ from the solubility parameter values is not refined enough for taking into account the various kinds of interactions (e.g., dispersive, dipole-dipole, hydrogens, etc.).

Another explanation is the presence of water clusters, which can be observed by dielectric measurements at high water uptake (Garden and Pethrick, 2017). The clustering function was defined by Zimm and Lundberg (1956) as:

$$f_{ZL} = \frac{G_{11}}{\nu_1} = -\left(1-\phi_1\right)\cdot\left[\frac{\partial a_1/\phi_1}{\partial a_1}\right]_{T,P} - 1 \tag{7.35}$$

When f_{ZL} is below a value of -1, no clustering occurs. Means cluster size (MCS) is given by:

$$\text{MCS} = 1 + \phi_1 \cdot G_{11}/\nu_{11} \tag{7.36}$$

It was, hence, shown (Davis and Elabd, 2013) that water molecules associate to form "dimers" when water external partial pressure (or activity) exceeds 0.2, which is typically the case when PMMA is immerged in water.

3. The Langmuir isotherm describes the equilibrium between the absorption (rate constant k_1) and desorption (rate constant $= k_{-1}$) of molecules on a surface; the rate being propositional to water external partial pressure (P) and the concentration of sorbed water (c), as described by:

$$k_1 \cdot P \cdot (1 - c) = k_{-1} \cdot c \tag{7.37}$$

which can be reformulated under the general form:

$$c = \frac{A \cdot p}{1 + B \cdot p} \tag{7.38}$$

In some cases, the sorption of a penetrant can be modeled by the dual sorption theory, which is the combination of Henry and Langmuir sorptions:

$$c = s \cdot p + \frac{A \cdot p}{1 + B \cdot p} \tag{7.39}$$

Some cases corresponding to this dual sorption mode are presented in Vieth et al. (1976).

There are several values for water-uptake in methacrylates immerged in water (Sideridou et al., 2003, 2008; Delpino Gonzales et al., 2016; Smith and Schmitz, 1988). Some of these are provided in Table 7.9.

The water affinity of a given polymer can be expressed as the number of water molecules absorbed per monomeric unit (Morel et al., 1985):

$$H = \frac{w_m \cdot M}{1800} = \sum n_i H_i \tag{7.40}$$

where M is the molar mass of the repetitive unit, n_i is the number of groups able to bind with H_i molecules of water.

Table 7.9 Water Equilibrium Mass Uptake in Several Methacrylate Polymers

		w/w	Reference
PMMA	23°C	1.90%	Smith and Schmitz (1988)
BisGMA	37°C	3.57%–3.86%	Sideridou et al. (2008)
TEGDMA	37°C	5.74% – 6.25%	Sideridou et al. (2008)
UDMA	37°C	2.39%–3.10%	Sideridou et al. (2008)
BisEMA	37°C	1.92%–2.11%	Sideridou et al. (2008)
D3MA	37°C	0.65%–0.66%	Sideridou et al. (2008)

H_i can be estimated from several polymers or chemicals (ideally with only one kind of functional group). For example, data for PMMA (Table 7.8) suggest $H_{\text{ester}} \sim 0.1$. However, this simple theory can fail for several reasons:

- The contribution of hydroxyl group (H_{OH}) might be weaker than in linear polymers such as PVOH because of the possibility of intramolecular hydrogen bonds (Kalachandra and Kusy, 1991) as observed when OH are hydrogen-bonded with heteroatoms (nitrogen atoms at the crosslink node for epoxy/diamine networks (Morel et al., 1985), oxygen for Bis-GMA.
- Water can have a very specific interaction with other water molecules (clustering).
- This simple theory considers the presence of polar and apolar groups, but not their molecular arrangements and the subsequent possibility to create "complexes" with water molecules.

Lastly, Kerby et al. (2009) also observed that the water uptake value is correlated with water contact angle: hydrophilic samples display a lower contact angle than hydrophobic ones.

7.5.2.2 Water diffusion

The diffusion of water in a polymer is expected to be described by the second Fick's law, provided that diffusivity does not depend on the water concentration:

$$\frac{\partial c}{\partial t} = D_w \cdot \frac{\partial^2 c}{\partial r^2} \tag{7.41}$$

This equation was solved analytically by Crank (1975), for example, in the case of an "infinite" plate having a $2e$ thickness:

$$\frac{m(t)-m_0}{m_\infty - m_0} = 1 - \frac{8}{\pi^2} \bullet \sum_{n=0}^{\infty} \frac{1}{(2n+1)^2} \bullet exp\left(- \frac{D \bullet (2n+1)^2 \bullet \pi^2 \bullet t}{4e^2} \right) \tag{7.42}$$

It is easy to verify that Eq. (7.42) describes fairly the sorption curves displayed in Fig. 7.19A. Increasing the number of terms of the index n allows a better description of the curve in the earliest sorption times.

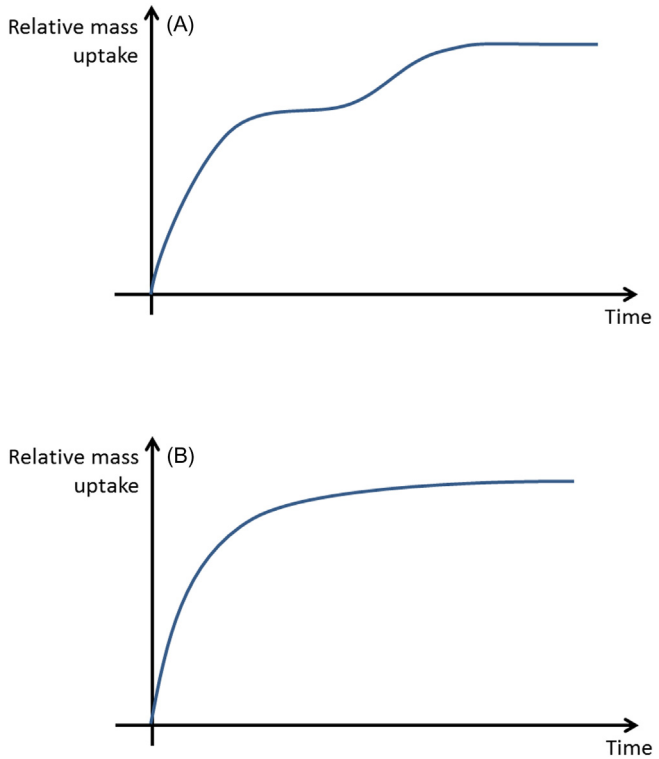

FIGURE 7.19

The general shape of mass uptake in a polymer in the presence of water in the case of a: (A) Fick Diffusion model; and (B) Langmuir diffusion model.

This equation can be simplified into:

- at low penetrant uptake ($m/m_\infty < 0{,}6$):

$$\frac{\Delta m(t)}{\Delta m_\infty} = \frac{4}{e} \bullet \sqrt{\frac{D \bullet t}{\pi}} \tag{7.43}$$

- at high penetrant uptake:

$$\frac{\Delta m(t)}{\Delta m_\infty} = 1 - \frac{8}{\pi^2} \bullet exp\left(- \frac{D\pi^2}{e^2} t \right) \tag{7.44}$$

In other words, if mass uptake varies linearly with the square root of time at low mass uptake values, it means that diffusion obeys Fick's law. The initial slope can, thus, be used to estimate the apparent diffusivity. It seems that the water diffusion into methacrylate-based polymers obeys Fick's law (Sideridou and Karabela, 2011; Barrie and Machin, 1971; Dhanpal et al., 2009;

Table 7.10 Values of Diffusion Coefficient in Several Resins (Sideridou and Karabela, 2011; Barrie and Machin, 1971)

	T (K)	D ($cm^2\ s^{-1}$)	Reference
PMMA	313.7	5.2×10^{-8}	Barrie and Machin (1971)
	323.4	8.9×10^{-8}	Barrie and Machin (1971)
	333	1.5×10^{-7}	Barrie and Machin (1971)
	343.2	2.4×10^{-7}	Barrie and Machin (1971)
BisGMA	310	1.1×10^{-7}	Sideridou and Karabela (2011)
BisEMA	310	0.74×10^{-7}	Sideridou and Karabela (2011)
UDMA	310	0.69×10^{-7}	Sideridou and Karabela (2011)
TEGDMA	310	0.15×10^{-7}	Sideridou and Karabela (2011)
D3MA	310	0.62×10^{-7}	Sideridou and Karabela (2011)

Sideridou et al., 2004). Some values are given in Table 7.10 that show differences between experiments performed in sorption mode compared to desorption mode (Sideridou and Karabela, 2011; Dhanpal et al., 2009; Sideridou et al., 2004).

Since samples actually differ from infinite plates (length [L] and width [l] are finite values), Shen and Springer (1976) proposed a correction for taking into account the geometry of samples:

$$D_{réel} = \frac{D_{app}}{\left(1 + \frac{2e}{L} + \frac{2e}{l}\right)^2} \tag{7.45}$$

D is expected to obey to Arrhenius law:

$$D(T) = D_0.exp\left(-\frac{E_D}{RT}\right) \tag{7.46}$$

In PMMA, E_D would be on the order of 45 kJ mol^{-1} (Barrie and Machin, 1971), which seems to be quite common with other values reported for amorphous polymers in their glassy state (Li et al., 2009b). Values slightly lower (30−35 kJ mol^{-1}) are observed in some matrices of dental composites (Dhanpal et al., 2009).

In some cases, the sorption curves display two plateaus which are attributed to the existence of polymeric sites inducing strong interactions with water molecules. Water molecules present in the polymer matrix divide into two parts:

- Free water which diffuses.
- Bound water being in strong interaction with some specific sites of the polymer.

This Langmuir-type diffusion was mathematically described by Carter and Kibler (1979) by denoting:

- $n(t)$ the concentration in "free" water.
- $N(t)$ the concentration in "bound" water.

- γ the probability that "free" water becomes "bound" water.
- β the probability that "bound" water becomes "free" water.

The equilibrium is described by:

$$\gamma \cdot n_\infty = \beta \cdot N_\infty \tag{7.47}$$

The system is described via a system of differential equations:

$$\frac{\partial n}{\partial t} + \frac{\partial N}{\partial t} = D \cdot \frac{\partial^2 n}{\partial x^2} \tag{7.48}$$

$$\frac{\partial N}{\partial t} = \gamma n - \beta N \tag{7.49}$$

By denoting:

$$\kappa = \frac{\pi^2 D}{(2e)^2} \tag{7.50}$$

Its solution can be approximated:

- at short absorption times:

$$\frac{N(t)}{N} = \frac{4}{\pi^{3/2}} \cdot \left(\frac{\beta}{\beta + \gamma}\right) \cdot \sqrt{\kappa t} \tag{7.51}$$

- at high absorption times:

$$\frac{N(t)}{N} = 1 - \frac{\gamma}{\beta + \gamma} \cdot \exp(-\beta t) \tag{7.52}$$

The "pseudo plateau" value can be approximated by:

$$\frac{N_{pseudo\ equilibre}}{N} = \frac{\beta}{\beta + \gamma} \tag{7.53}$$

However, such a process has not been reported, to the best of our knowledge, for the case of any methacrylate-based materials.

The rate at which water diffuses is influenced by the penetrant architecture and polymer free volume, as proposed by Cohen and Turnbull (1959):

$$D = D_0 \cdot \exp\left(-b/V_f\right) \tag{7.54}$$

where, b is related to penetrant size and V_f to polymer "empty" space allowing penetrant jumps.

"Free volume" theory is, for example, well-illustrated in the case of epoxy networks when correlating the measured value of diffusivity (determined from the classical gravimetric method) with the volume of nanoholes (expected to be linked to free volume) (Frank and Wiggins, 2013). In the case of methacrylate-based polymers, it was observed that the diffusivity values in networks-based tetrafunctional methacrylates was lower than in analogous methacrylates, presumably because of the highly crosslinked nature of the networks and the lower free-volume content (Kalachandra and Kusy, 1991).

Theories linking diffusivity with the capability of polymer segments to facilitate diffusion are also illustrated in polymers having a subglassy transition (also named β transition) where Halary observed a good correlation between the occurrence of this transition and the diffusivity of water (Halary, 2000).

It seems, also, that the ageing by physical relaxation (see Section 7.5.1) can influence the overall-water ageing process, since the decrease in free volume is accompanied by an overall lower penetration of water, as illustrated by Siu-Wai Kong (1986) in the case of epoxies resins.

Contrarily to theories considering diffusion being mainly influenced by the amount of free volume, Verdu and colleagues (Merdas et al., 2002) observed that for a family of epoxy resins, diffusivity was inversely correlated with solubility. Since this later mainly originated from polar groups (such as isopropanol in epoxies) inducing a strong interaction with water, they suggested that these later decrease the diffusivity. The following mechanism was proposed:

$[P_1 \ldots W] \rightarrow P_1 + W$	Dissociation of water/polymer complex
$W \rightarrow$	Jump of a water molecule from P_1 to P_2
$W + P_2 \rightarrow [P_2 \ldots W]$	Formation of a new water/polymer complex

This theory is verified in part by Dhanpal et al. (2009) for some dental composites, where the differences are few.

7.5.2.3 Consequences of physical ageing on mechanical properties

Water is a small molecule characterized by a low T_g ($T_g = 136$K for water; Angell et al., 1978). It is, thus, not surprising that the main consequence of water penetration in acrylate polymers is a decrease of glass transition temperature (Smith and Schmitz, 1988), which can be tentatively described by several models, such as:

1. The DiMarzio's equation is the simplest law for describing the T_g depletion for a polymer in presence of a plasticizer:

$$\frac{1}{T_g} = \frac{w_1}{T_{g1}} + \frac{w_2}{T_{g2}} \tag{7.55}$$

2. A thermodynamic theory was proposed by Couchmann and Karasz (ten Brinke et al., 1983):

$$\ln T_g = \frac{w_1 \cdot \Delta C_{p1} \cdot ln T_{g1} + w_2 \cdot \Delta C_{p2} \cdot ln T_{g2}}{w_1 \cdot \Delta C_{p1} + w_2 \cdot \Delta C_{p2}} \tag{7.56}$$

where ΔC_p is change of heat capacity at T_g for each component of the mixture equal to $\Delta C_{P1} = 1.94$ J (g K)$^{-1}$ for PMMA and $\Delta C_{P2} = 0.318$ J (g K)$^{-1}$ for water.

3. Ellis and Karasz (1984):

$$T_g = \frac{w_1 \cdot \Delta C_{p1} \cdot T_{g1} + w_2 \cdot \Delta C_{p2} \cdot T_{g2}}{w_1 \cdot \Delta C_{p1} + w_2 \cdot \Delta C_{p2}} \tag{7.57}$$

4. Kelley and Bueche (1961):

$$T_g = \frac{\Delta\alpha \cdot T_{g2} \cdot \phi_2 + \alpha_1 \cdot T_{g1} \cdot \phi_1}{\Delta\alpha \cdot \phi_2 + \alpha_1 \phi_1} \tag{7.58}$$

where α_1 is the diluent coefficient of cubic expansion, and $\Delta\alpha$ is the change of coefficient of cubic expansion for the polymer at T_g for which it is considered as an universal value close to 4.8×10^{-4} K^{-1}.

The effect of water absorption in PMMA is illustrated on the depletion of elasticity modulus in the glassy state from 3700 to 3000 MPa when water fraction increases from 0% to 1.4% (Delpino Gonzales et al., 2016).

$$T_g = \frac{f \cdot w_1 \cdot \Delta C_{p1} \cdot T_{g1} + w_2 \cdot \Delta C_{p2} \cdot T_{g2}}{f \cdot w_1 \cdot \Delta C_{p1} + w_2 \cdot \Delta C_{p2}} \tag{7.59}$$

where f is considered as the fraction of water active for reducing T_g (i.e., $1 - f$ is the fraction of water absorbed in microvoids).

In fully cured networks, water plasticization results in a decrease in compressive strength and microhardness (Ferracane et al., 1998; Kalliyana Krishnan et al., 1997). A good illustration is given in the case of Bis-GMA + HEMA networks in Park et al. (2009), the results of which are schematized in Fig. 7.20.

According to the Kambour's theory, yield stress depends on the value of T_g (see Section 7.4.1). A decrease in glass transition results in a decrease in yield stress as illustrated by Leger et al. (2013): according to these authors, changes in mechanical properties induced by solvent ingress leading to a given temperature decrease (e.g., 20°C) are equivalent to the mechanical properties decrease induced by the same temperature increase (i.e. 20°C).

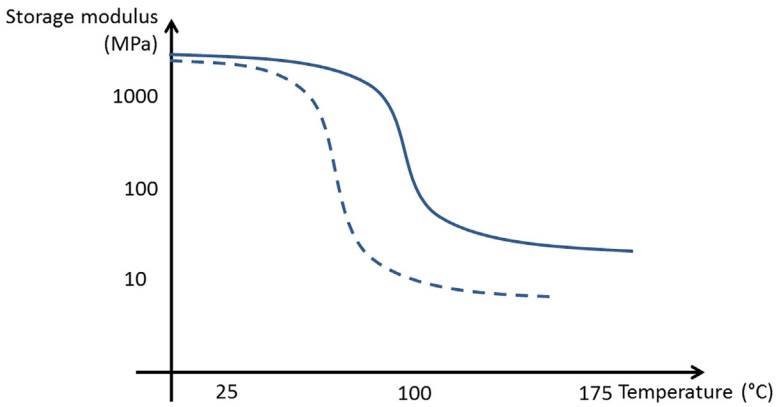

FIGURE 7.20

Schematic thermomechanical behavior of virgin (full line) and water-aged (dashed line) bis-GMA + HEMA resin (in the case of physical ageing without chemical reactions).

It is worth noting that physical ageing is, in principle, characterized by an equilibrium state, i.e., physical properties are expected to plateau after a long-exposure time. However, since dental composites are sometimes undercured, the decrease in T_g and subsequent macromolecular mobility increase may also induce an increase in conversion degree and later in some mechanical properties (Ferracane et al., 1998; Malacarne-Zanon et al., 2009).

7.5.2.4 Role of the interface

A supplementary level of complexification is observed in composites. It was also observed that the polymer/fillers interface displays usually weaker properties than the "bulky" polymer matrix, as illustrated in numerous papers dealing with T_g measurements of organic matrices at the boundary with the interface (Tillman et al., 2002; Joliff et al., 2013). It is, thus, observed that water solubility and diffusivity in composites are higher than those predicted by a simple mixture law (i.e., assuming that water does not diffuse into the filler) as observed by Chateauminois et al. (1994) in the case of reinforced epoxies.

This was also illustrated by Kalachandra (1989) in the case of PMMA filled with barium-based particles (Table 7.11). The detrimental effects of the interface can be partially attenuated by the use of proper coupling agents (such as 4-methacryloxyethyl trimellitic anhydride).

Other examples are reported for the case of dimethacrylates used in dentistry where:

- Water solubility reaches 1.2%−1.7% even for composites with c. 75% weight fillers (Wei et al., 2011), that is, higher than expected from the water-uptake value for pure resin (see Table 7.8).
- The diffusivity is observed to be higher in composites than in the pure matrix (Dhanpal et al., 2009).

Table 7.11 Water Sorption Parameter at 37°C in PMMA and Its Composites

Material	% Polymer	Diffusion Coefficient ($\times 10^8$ cm^2 s^{-1})	% Water Uptake	
			Calulated	Experimental
PMMA	100	2.26		2.28
PMMA + barium sulfate	31	33.18	0.71	1.23
PMMA + barium sulfate + coupling agent	30	10.08	0.68	1.27
PMMA + barium glass silance coated	25	10.55	0.57	1.23
PMMA + barium glass silance coated + coupling agent	23	9.42	0.52	1.04

The water solubility and/or diffusivity are higher than in the pure matrix, thus, needing a much more complex modeling (Joliff et al., 2014).

In terms of mechanical properties, these observations are consistent with the results obtained by Jager et al. (2016a) who found highly filled matrices to be the most sensitive to water permeation.

7.5.2.5 Effect of penetrant composition mixture

It seems that, in a first approach, water has almost the same effect than various artificial salivas, as illustrated by Al-Mulla et al. (1989).

Ethanol is also more soluble in dimethacrylates than water (Malacarne-Zanon et al., 2009), consistent with its lower solubility parameter (26.5 $MPa^{1/2}$) than water.

The effect of water and more acidic media (coke, orange juice) was compared by Rahim et al. (2012) showing that:

- Diffusion mechanism remains Fickian in every case.
- The water diffusion coefficient remains about constant.
- The maximum fluid uptake and the fraction of solubilized compounds increases. This last result can be explained due to better leaching of unreacted monomers and soluble materials and/or a possible hydrolysis reaction, which will be next.

7.5.3 CHEMICAL AGEING BY HYDROLYSIS

A supplementary effect of water penetration is the possible hydrolysis of ester groups. In the case of biomaterials, these reactions were proposed:

1. In the case of PMMA where chain scission occur on side chains (Ayre et al., 2014; Ali et al., 2015; Semen and Lando, 1969; Du et al., 2006) (Scheme 7.9). The hydrolytic degradation is, thus, expected to firstly modify the polarity of the material (since each elementary reaction converts one ester group into a carboxylic acid group).
2. In the case of TEGDMA in the presence of enzymes such as cholesterol esterase (Ferracane, 2006; Finer and Santerre, 2004) (Scheme 7.10).

In ideal networks (no dangling chains or loops), one has:

$$n = n_0 - 3s \tag{7.60}$$

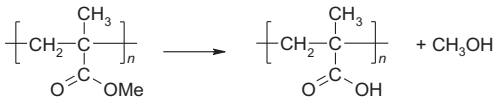

SCHEME 7.9

Mechanism of PMMA hydrolysis.

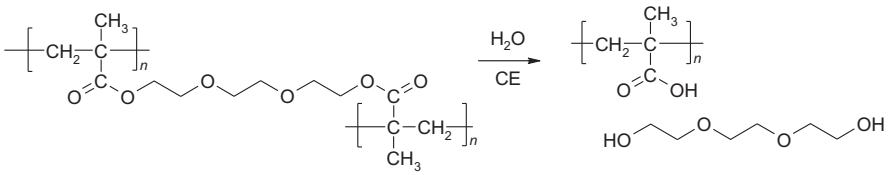

SCHEME 7.10

Mechanism of TEGDMA hydrolysis.

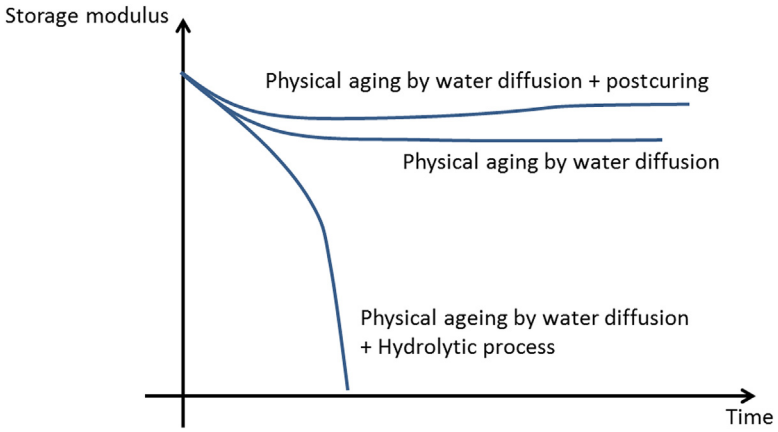

FIGURE 7.21

Typical kinetic curves for various ageing processes involving water.

But, this relation is no longer valid when networks differ from the ideal (since each chain scission generates two dangling chains). The complete mathematical treatment is proposed in Richaud et al. (2014).

In networks such as Bis-GMA, the ratio of ester bond needed for the "degelation" of the network (i.e., the total disappearance of elastically active chains and the possible solubilization of the material in a good solvent) is given by (Gilormini et al., 2014):

$$x_d = 1 - \frac{1}{\sqrt{1 + \frac{2}{L}}} \tag{7.61}$$

L being the number of reactive units (here hydrolysable ester groups) per elastic chain.

Since carboxylic acids are efficient catalysts of the hydrolysis reaction, the hydrolysis degradation can display a certain autoaccelerated behavior (Richaud et al., 2014). The kinetic aspects of ageing are depicted in Fig. 7.21.

Lastly, it must be mentioned that the kinetics of water ageing may be controlled by the rate of water diffusion from the edge to the bulk (El Yagoubi et al., 2012). This means that the general equation for water consumption in any layer of the polymer is given by (Jacques et al., 2002):

$$\frac{\partial w}{\partial t} = D_w \cdot \frac{\partial^2 w}{\partial x^2} - k_h \cdot w \cdot e \tag{7.62}$$

where D_w is the water diffusivity, k_h is the rate constant for hydrolysis, e and w are, respectively, the concentrations in water and in hydrolysable groups (namely ester).

This equation can be adapted for several practical cases (e.g., the existence of several kinds of reactive groups, or the possibility of noncatalyzed and catalyzed hydrolysis), but in the simplest case, the thickness of degraded layer can be approximated by:

$$z_{degraded} = \sqrt{\frac{D_w \cdot w_s}{k_h}} \tag{7.63}$$

In other words, the final properties of the polymer correspond to the average of the undegraded bulk and the degraded edges.

7.5.4 CHEMICAL AGEING BY RADIOLYSIS

Radiolytic processes are involved in the sterilization of some polymers before implantation (Barton et al., 2013). Results obtained on PMMA unambiguously show the decrease of molar mass, which is ascribed to the mechanisms shown in Scheme 7.11.

The number of scissions induced by an irradiation dose D per unit mass is given by:

$$s = G(s) \cdot D \tag{7.64}$$

where $G(s)$ denotes the radiochemical yield of PMMA (in mol J^{-1}). The radiochemical yield $G(s)$ should be close to $1-2 \times 10^{-7}$ mol J^{-1} in PMMA (Schnabel, 1978; Thominette et al., 1989; Babu et al., 1984; Charlesby and Moore, 1964). Even if it is not of clinical interest, the case of the radiolysis of networks obtained from dimethacrylate remains an open question since the reactivity of esters (i.e., the radiochemical yield for chain scission) present in dimethacrylate might differ from the reactivity of esters present in PMMA (Gilormini et al., 2017).

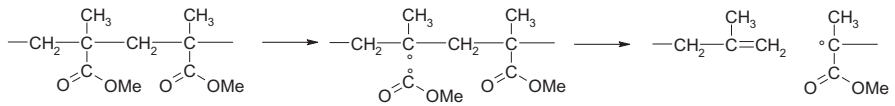

SCHEME 7.11

The mechanisms of chain scission in PMMA.

7.5.5 CREEP AND FATIGUE

Let us first recall that there are two kinds of fatigue experiments:

1. Those made on unnotched samples: they lead to Wohler curves where mechanical stress is plotted versus the number of cycles. The Wohler curves of bulk- and reinforced-PMMA are compared in Baleani et al. (2003). The report shows that filler would have a detrimental effect on fatigue resistance.
2. Those made on notched samples (fatigue crack propagation): they lead to the plot of crack growth rate (da/dN) versus the intensity factor ($\Delta K = \Delta\sigma \cdot a \cdot \pi^{1/2} \cdot f = K_{\max} - K_{\min}$, $K_{\max}$, and $K_{\min}$ are defined as the maximum and minimum stress intensity experienced by the crack and f being a geometric factor). The classical curve for fatigue crack propagation is depicted in Fig. 7.22.

The left side of the curve leads to the minimal value of stress intensity factor (also named fatigue crack inception or threshold ΔK_i or ΔK_{th}) leading to crack propagation. Higher values of ΔK_i correspond to tougher samples. ΔK_i is slightly higher than 0.1 MPa $m^{1/2}$ in PMMA (Ramsteiner and Armbrust, 2001) and c. five-times higher for composites used in dental restoration (Shah et al., 2009).

The right side of the curve is a vertical asymptote reached at a stress intensity value K_C close to the sample toughness (see Section 7.4.1) and linked to the critical size of a defect leading to brittle failure:

$$a_C = \frac{1}{\pi} \cdot \sqrt{\frac{K_C}{\Delta\sigma}} \tag{7.65}$$

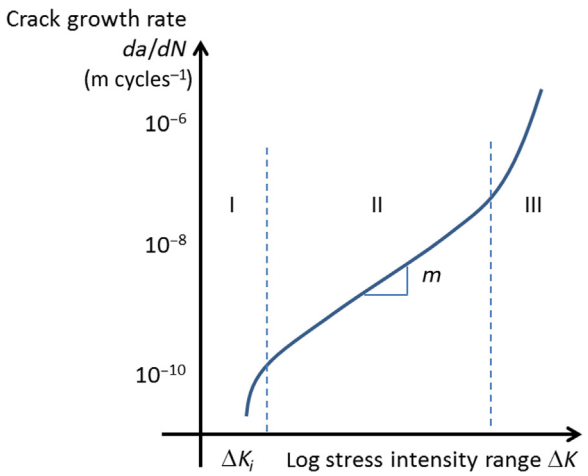

FIGURE 7.22

Schematic results of fatigue crack propagation experiment.

In the intermediary domain, a linear dependence between crack growth rate and stress intensity factor is observed, which is described by the Paris law (Paris et al., 1961):

$$\frac{da}{dN} = C \cdot \Delta K^m \tag{7.66}$$

In the case of thermoplastic polymers, the positive effect of average molar mass is illustrated in Skibo et al. (1977). The most probable explanation is that longer polymer chains produce effective entanglements and better fatigue resistance of the crazes.

Fig. 7.23 illustrates a comparison of crack growth rate on PMMA aged in air and that grown in a Ringer solution (Ayre et al., 2014) and illustrates the complexities of the effect of ageing on fatigue properties. m would be on the order of 5 for hydrolytically aged dental composites made of Bis-GMA, UDMA, Bis-EMA, and a small amount of TEGDMA, together with 60% of silica and zirconia fillers. Moreover, SEM observations show that the cracks propagate at the particle matrix interface and cause possible matrix-filler debonding (Shah et al., 2009).

From a practical point of view, it is noteworthy that polymers are bad thermal conductive materials and that a high frequency for fatigue test can induce significant self-heating. Temperature can for example exceed 100°C in a PMMA submitted to a 50 Hz cyclic stress, meaning that sample reaches is rubbery domain and sample fails at a very low number of cycles (Justice and Schultz, 1980).

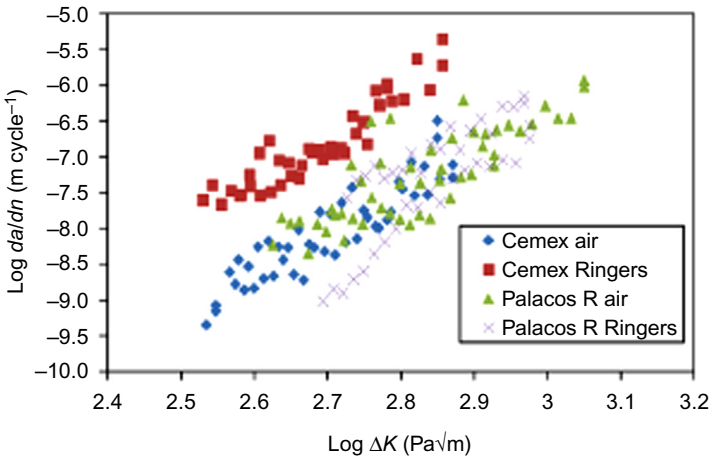

FIGURE 7.23

Crack growth rate of a PMMA bone cement aged in air or in Ringer's solution

7.6 CONCLUSION AND PROSPECTS FOR THE FUTURE OF THESE MATERIALS

PMMA and methacrylates polymers are easily obtained by radical in-chain polymerization which makes composites easy to use for surgeons and dentists as biomaterials and matrices.

In this chapter, we presented various methods for synthesis and the structure-properties relationships aimed for designing materials.

However, they are sensitive, in particular, to water resulting that the initial properties cannot be maintained in vivo. The main degradation mechanisms expected to occur at moderate temperature, during use or sterilization by irradiation were presented and might be helpful to avoid complications induced by long-term ageing. One of the scientific challenges remains to take into account the presence of fillers complicating the lifetime prediction.

In the future, researches should pursue improving the dispersion of fillers and the development of materials that offer a good compromise between low viscosity and improved mechanical properties. The properties could also be improved by new polymerization strategies involving, for example, enhanced hydrostatic pressure to limit the presence of porosities which are known to dramatically decrease the mechanical properties of composites and increasing composites' water uptake (Soles et al., 2000).

REFERENCES

Al-Mulla, M.A.S., Murphy, W.M., Huggett, R., Brooks, S.C., 1989. Effect of water and artificial saliva on mechanical properties of some denture-base materials. Dent. Mater. 5 (6), 399–402.

Ali, U., Karim, K.J.B.A., Buang, N.A., 2015. A review of the properties and applications of poly (methylmethacrylate) (PMMA). Polym. Rev. 55 (4), 678–705.

Aljabo, A., Xia, W., Liaqat, S., Khan, M.A., Knowles, J.C., Ashley, P., et al., November 2015. Conversion, shrinkage, water sorption, flexural strength and modulus of re-mineralizing dental composites. Dent. Mater. 31 (11), 1279–1289.

Angell, C.A., Sare, J.M., Sare, E.J., 1978. Glass transition temperatures for simple molecular liquids and their binary solutions. J. Phys. Chem. 82 (24), 2622–2629. Available from: https://doi.org/10.1021/j100513a016.

Arnold, J.C., 1995. The effects of physical aging on the brittle fracture behavior of polymers. Polym. Eng. Sci. 35 (2), 165–169.

Asgharzadeh Shirazi, H., Mirmohammadi, S.A., Shaali, M., Asnafi, A., Ayatollahi, M.R., 2017. A constitutive material model for a commercial PMMA bone cement using a combination of nano-indentation test and finite element analysis. Polym. Test. 59, 328–335.

Atai, M., Pahlavan, A., Moin, N., 2012. Nano-porous thermally sintered nano silica as novel fillers for dental composites. Dent. Mater. 28 (2), 133–145.

Ayre, W.N., Denyer, S.P., Evans, S.L., 2014. Ageing and moisture uptake in polymethyl methacrylate (PMMA) bone cements. J. Mech. Behav. Biomed. Mater. 32, 76–88.
Babu, G.N., Narula, A., Hsu, S.L., Chien, J.C.W., 1984. Radiolysis of resist polymers. 1. Poly(methyl α-haloacrylates) and copolymers with methyl methacrylate. Macromolecules 17, 2749–2755.
Bala, O., Olmez, A., Kalayci, S., 2005. Effect of LED and halogen light curing on polymerization of resin-based composites. J. Oral Rehab. 32 (2), 134–140.
Baleani, M., Cristofolini, L., Minari, C., Toni, A., 2003. Fatigue strength of PMMA bone cement mixed with gentamicin and barium sulphate vs pure PMMA. Proc. Inst. Mech. Eng., Part H: J. Eng. Med. 217 (1), 9–12.
Ballo, A., Närhi, T., 2017. Biocompatibility of fiber-reinforced composites for dental applications. Biocompat. Dent. Biomater. 23–39.
Balthazard, R., Jager, S., Dahoun, A., Gerdolle, D., Engels-Deutsch, M., Mortier, E., 2014. High-resolution tomography study of the porosity of three restorative resin composites. Clin. Oral Invest. 18 (6), 1613–1618.
Barrie, J.A., Machin, D., 1971. Diffusion and association of water in some polyalkylmethacrylates. Part 1 – Equilibrium sorption and steady state permeation. Trans. Faraday Soc. 67, 244–256.
Barszczewska-Rybarek, I.M., 2009. Structure–property relationships in dimethacrylate networks based on Bis-GMA, UDMA and TEGDMA. Dent. Mater. 25, 1082–1089.
Barton, S.J., Foot, P.J.S., Miller Tate, P.C., Kishi, M., Ghatora, B., 2013. The effects of gamma irradiation on medical grade poly(methyl methacrylate). Polym. Polym. Compos. 21 (1), 1–8.
Baskaran, D., Müller, A.H.E., 2007. Anionic vinyl polymerization—50 years after Michael Szwarc. Prog. Polym. Sci. 32 (2), 173–219.
Begum, F., Simon, S.L., 2011. Modeling methyl methacrylate free radical polymerization in nanoporous confinement. Polymer 52 (7), 1539–1545.
Begum, F., Zhao, H., Simon, S.L., 2012. Modeling methyl methacrylate free radical polymerization: Reaction in hydrophobic nanopores. Polymer 53 (15), 3261–3268.
Bellenger, V., Verdu, J., Morel, E., 1987. Effect of structure on glass transition temperature of amine crosslinked epoxies. J. Polym. Sci., Part B: Polym. Phys. 25 (6), 1219–1234.
Bergmann, C.P., Stumpf, A., 2013. Dental Ceramics Microstructure, Properties and Degradation, Topics in Mining, Metallurgy and Materials Engineering. Springer-Verlag Berlin Heidelberg.
Bhamra, G.S., Fleming, G.J.P., Darvell, B.W., 2010. Influence of LED irradiance on flexural properties and Vickers hardness of resin-based composite materials. Dent. Mater. 26 (2), 148–155.
Bindu, M.G., Satapathy, B.K., Jaggi, H.S., Ray, A.R., 2013. Size-scale effects of silica on bis-GMA/TEGDMA based nanohybrid dental restorative composites. Compos. Part B 53, 92–102.
Bocalon, A.C.E., Mita, D., Narumyia, I., Shouha, P., Xavier, T.A., Braga, R.R., 2016. Replacement of glass particles by multidirectional short glass fibers in experimental composites: Effects on degree of conversion, mechanical properties and polymerization shrinkage. Dent. Mater. 32 (9), 204–210.
Bowen, R.L., 1962. Dental Filing Material Comprising Vinyl Silane Treated Fused Silica and a Binder Consisting of the Reaction Product of Bis Phenol and Glycidyl Acrylate. US Patent 3,066,112.

Buonocore, M.G., 1955. A simple method of increasing the adhesion of acrylic filling materials to enamel surfaces. J. Dent. Res. 34 (6), 849–853.
Cardenas, J.N., O'Driscoll, K.F., 1976. High-conversion polymerization. I. Theory and application to methyl methacrylate. J. Polym. Sci.: Polym. Chem. Ed. 14, 883–897.
Carter, H.G., Kibler, K.G., 1979. Langmuir-type Model anomalous moisture diffusion in composite resins. J Compos. Mater. 12, 118–130.
Charlesby, A., Moore, N., 1964. Comparison of gamma and ultra-violet radiation effects in polymethyl methacrylate at higher temperatures. Int. J. Appl. Radiat. Isot. 15, 703–708.
Chateauminois, A., Vincent, L., Chabert, B., Soulier, J.P., 1994. Study of the interfacial degradation of a glass-epoxy composite during hygrothermal ageing using water diffusion measurements and dynamic mechanical thermal analysis. Polymer 35 (22), 4766–4774.
Chi Phan, A., Béhin, P., Stoclet, G., Ruse, N.D., Nguyen, J.-F., Sadoun, M., April 2015. Optimum pressure for the high-pressure polymerization of urethane dimethacrylate. Dent. Mater. 31 (4), 406–412.
Chunga, S.M., Yapa, A.U.J., Kohb, W.K., Tsaic, K.T., Limd, C.T., 2004. Measurement of Poisson's ratio of dental composite restorative materials. Biomaterials 25, 2455–2460.
Cohen, M.H., Turnbull, D., 1959. Molecular transport in liquids and glasses. J. Chem. Phys. 31 (5), 1164–1169.
Cokic, S.M., Hoet, P., Godderis, L., Wiemann, M., Asbach, C., Reichl, F.X., et al., 2016. Cytotoxic effects of composite dust on human bronchial epithelial cells. Dent. Mater. 32 (12), 1482–1491.
Cooke, W.D., Mayr, A.E., Edwards, G.H., 1998. Yielding behaviour in model thermosets – II. Temperature dependence. Polymer 39 (16), 3725–3733.
Crank, J., 1975. The Mathematics of Diffusion, second ed. Clarenson Press, Oxford (Chapter xxxx).
Davis, E.M., Elabd, Y.A., 2013. Water clustering in glassy polymers. J. Phys. Chem. B 117 (36), 10629–10640.
Delpino Gonzales, O., Nicassio, A., Eliasson, V., 2016. Evaluation of the effect of water content on the stress optical coefficient in PMMA. Polym. Test. 50, 119–124.
Dewaele, M., Asmussen, E., Peutzfeldt, A., Munksgaard, E.C., Benetti, A.R., Finné, G., et al., 2009. Influence of curing protocol on selected properties of light-curing polymers: degree of conversion, volume contraction, elastic modulus, and glass transition temperature. Dent. Mater. 25 (12), 1576–1584.
Dhanpal, P., Yiu, C.K.Y., King, N.M., Tay, F.R., Hiraishi, N., 2009. Effect of temperature on water sorption and solubility of dental adhesive resins. J. Dent. 37 (2), 122–132.
DiMarzio, E.A., 1964. On the second-order transition of a rubber. J. Res. Natl. Bureau Standards: Sect. A: Phys. Chem. 68, 611–617.
Diaz-Calleja, R., Perez, J., Gomez-Ribelles, J.L., Ribes-Greus, A., 1987. Physical model explaining the effect of physical ageing on dynamic mechanical and calorimetric properties of poly (Methyl Methacrylate). Macromol. Symp. 27, 289–297.
Du, X.-W., Fu, Y.-S., Sun, J., Han, X., Liu, J., 2006. Complete UV emission of ZnO nanoparticles in a PMMA matrix. Semicond. Sci. Technol. 21 (8), 1202–1206.
Dušek, K., 1996. Diffusion control in the kinetics of cross-linking. Polym. Gels Networks 4 (5–6), 383–404.
El Yagoubi, J., Lubineau, G., Roger, F., Verdu, J., 2012. A fully coupled diffusion-reaction scheme for moisture sorptionedesorption in an anhydride-cured epoxy resin. Polymer 53 (24), 5582–5595.

Elliott, J.E., Lovell, L.G., Bowman, C.N., 2001. Primary cyclization in the polymerization of bis-GMA and TEGDMA: a modeling approach to understanding the cure of dental resins. Dent. Mater. 17 (3), 221–229.
Ellis, T.S., Karasz, F.E., 1984. Interaction of epoxy resins with water: the depression of glass transition temperature. Polymer 25 (5), 664–669.
Ernault, E., Richaud, E., Fayolle, B., 2017. Thermal-oxidation of epoxy/amine followed by glass transition temperature changes. Polym. Degrad. Stabil. 138, 82–90.
Etienne, S., Hazeg, N., Duval, E., Mermet, A., Wypych, A., David, L., 2007. Physical aging and molecular mobility of amorphous polymers. J. Non-Crystalline Solids 353 (41–43), 3871–3878.
Ferracane, J.L., 2005. Developing a more complete understanding of stresses produced in dental composites during polymerization. Dent. Mater. 21 (1), 36–42.
Ferracane, J.L., 2006. Hygroscopic and hydrolytic effects in dental polymer networks. Dent. Mater. 22 (3), 211–222.
Ferracane, J.L., 2011. Resin composite – state of the art. Dent. Mater. 27 (1), 29–38.
Ferracane, J.L., Mitchem, J.C., Condon, J.R., Todd, R., 1997. Wear and marginal breakdown of composites with various degrees of cure. J. Dent. Res. 76 (8), 1508–1516.
Ferracane, J.L., Berge, H.X., Condon, J.R., 1998. In vitro aging of dental composites in water--effect of degree of conversion, filler volume, and filler/matrix coupling. J. Biomed. Mater. Res. 42 (5), 465–472.
Finer, Y., Santerre, J.P., 2004. Salivary esterase activity and its association with the biodegradation of dental composites. J. Dent. Res. 83 (11), 22–26.
Floyd, C.J., Dickens, S.H., 2006. Network structure of Bis-GMA- and UDMA-based resin systems. Dent. Mater. 22 (12), 1143–1149.
Fonseca, A.S., Labruna Moreira, A.D., de Albuquerque, P.P., de Menezes, L.R., Pfeifer, C. S., Schneider, L.F., 2017. Effect of monomer type on the C = C degree of conversion, water sorption and solubility, and color stability of model dental composites. Dent. Mater. 33 (4), 394–401.
Foroutan, F., Javadpour, J., Khavandi, A., Atai, M., Rezaie, H.R., 2011. Mechanical properties of dental composite materials reinforced with micro and nano-size Al_2O_3 filler particles. Iran. J. Mater. Sci. Eng. 8 (2), 25–33.
Foster, J., Walker, R., Inventors, 1974. United States Patent Office 32825@518 3,825,518 DENTAL F'ILLING MATERUM. US patent.
Fox Jr., T.G., Flory, P.J., 1950. Second-order transition temperatures and related properties of polystyrene. I. Influence of molecular weight. J. Appl. Phys. 21 (6), 581–591.
Frank, K., Wiggins, J., 2013. Effect of stoichiometry and cure prescription on fluid ingress in epoxy networks. J. Appl. Polym. Sci. 130 (1), 264–276.
Garden, L., Pethrick, R.A., 2017. A dielectric study of water uptake in epoxy resin systems. J. Appl. Polym. Sci. 134 (16).
Gatti, A.M., 2004. Biocompatibility of micro- and nano-particles in the colon. Part II. Biomaterials 25 (3), 385–392.
Gatti, A.M., Rivasi, F., 2002. Biocompatibility of micro- and nanoparticles. Part I: In liver and kidney. Biomaterials 23 (11), 2381–2387.
Gilbert, D.G., Ashby, M.F., Beaumont, P.W.R., 1986. Modulus-maps for amorphous polymers. J. Mater. Sci. 21, 3194–3210.
Gilormini, P., Richaud, E., Verdu, J., 2014. A statistical theory of polymer network degradation. Polymer 55 (16), 3811–3817.

Gilormini, P., Richaud, E., Verdu, J., 2017. Radiochemical “degelation” of polymethyl methacrylate networks. Polymer 111, 130–136.
Grassia, L., D’Amore, A., 2011. Isobaric and isothermal glass transition of PMMA: pressure-volume-temperature experiments and modelling predictions. J. Non-Crystalline Solids 357 (2), 414–418.
Grassia, L., Simon, S.L., 2012. Modeling volume relaxation of amorphous polymers: Modification of the equation for the relaxation time in the KAHR model. Polymer 53 (16), 3613–3620.
Guth, E., 1945. Theory of filler reinforcement. J. Appl. Phys. 16 (1), 20–25.
Haenel, T., Hausnerová, B., Steinhaus, J., Price, R.B., Sullivan, B., Moeginger, B., 2015. Effect of the irradiance distribution from light curing units on the local micro-hardness of the surface of dental resins. Dent. Mater. 31 (2), 93–104.
Halary, J.L., 2000. Structure-property relationships in epoxy-amine networks of well-controlled architecture. High Performance Polym. 12, 141–153.
Halpin, J.C., Kardos, J.L., 1976. The Halpin-Tsai equations: a review. Polym. Eng. Sci. 16 (5), 344–352.
Heintze, S.D., 2006. How to qualify and validate wear simulation devices and methods. Dent. Mater. 22 (8), 712–734.
Hodge, I.M., 1994. Enthalpy relaxation and recovery in amorphous materials. J. Non-Crystalline Solids 169 (3), 211–266.
Hutchinson, J.M., Bucknall, C.B., 1980. The effects of thermal history on the density and mechanical properties of poly(methyl methacrylate). Polym. Eng. Sci. 20 (3), 173–181.
Ihara, E., Omura, N., Itoh, T., Inoue, K., 2007. Anionic polymerization of methyl methacrylate and tert-butyl acrylate initiated with the YCl_3/lithium amide/nBuLi systems. J. Organomet. Chem. 692 (1–3), 698–704.
Ilie, N., Hickel, R., 2011. Resin composite restorative materials. Aust. Dent. J. 56 (Suppl. 1), 59–66.
Issa, Y., Watts, D.C., Boyd, D., Price, R.B., 2016. Effect of curing light emission spectrum on the nanohardness and elastic modulus of two bulk-fill resin composites. Dent. Mater. 32 (4), 535–550.
Jacques, B., Werth, M., Merdas, I., Thominette, F., Verdu, J., 2002. Hydrolytic ageing of polyamide 11. 1. Hydrolysis kinetics in water. Polymer 43 (24), 6439–6447.
Jager, S., Balthazard, R., Dahoun, A., Mortier, E., 2016a. Filler content, surface microhardness, and rheological properties of various flowable resin composites. Operat. Dent. 41 (6), 655–665.
Jager, S., Balthazard, R., Vincent, M., Dahoun, A., Mortier, E., 2016b. Dynamic thermomechanical properties of various flowable resin composites. J. Clin. Exp. Dent. 8 (5), 534–539.
Joliff, Y., Belec, L., Chailan, J.F., 2013. Modified water diffusion kinetics in an unidirectional glass/fibre composite due to the interphase area: Experimental, analytical and numerical approach. Compos. Struct. 97, 296–303.
Joliff, Y., Rekik, W., Belec, L., Chailan, J.F., 2014. Study of the moisture/stress effects on glass fibre/epoxy composite and the impact of the interphase area. Compos. Struct. 108, 876–885.
Justice, L.A., Schultz, J.M., 1980. Enhancement of the fatigue life of PMMA through prior crazing. J. Mater. Sci. 15 (6), 1584–1585.

Kalachandra, S., 1989. Influence of fillers on the water sorption of composites. Dent. Mater. 5 (4), 283–288.
Kalachandra, S., Kusy, R.P., 1991. Comparison of water sorption by methacrylate and dimethacrylate monomers and their corresponding polymers. Polymer 32 (13), 2428–2434.
Kalliyana Krishnan, V., Manjusha, K., Yamuna, V., 1997. Effect of diluent upon the properties of a visiblelight-cured dental composite. J. Mater. Sci.: Mater. Med. 8, 703–706.
Kardos, J.L., 1993. Short-fiber-reinforced polymeric composites, structure–property relations. In: Lee, S.M. (Ed.), Handbook of Composites. Wiley-VCH, Palo Alto, CA, p. 593.
Kelley, F.N., Bueche, F., 1961. Viscosity and glass temperature relations for polymer-diluent systems. J. Polym. Sci. 50 (154), 549–556.
Kerby, R.E., Knobloch, L.A., Schricker, S., Gregg, B., 2009. Synthesis and evaluation of modified urethane dimethacrylate resins with reduced water sorption and solubility. Dent. Mater. 25 (3), 302–313.
Khandaker, M., Meng, Z., 2015. The effect of nanoparticles and alternative monomer on the exothermic temperature of PMMA bone cement. Procedia Eng. 105, 946–952.
Kleverlaan, C.J., Feilzer, A.J., 2005. Polymerization shrinkage and contraction stress of dental resin composites. Dent. Mater. 21 (12), 1150–1157.
Lalande, L., Plummer, C.J.G., Månsona, J.-A.E., Gérard, P., 2006. Microdeformation mechanisms in rubber toughened PMMA and PMMA-based copolymers. Eng. Fract. Mech. 73 (16), 2413–2426.
Leger, R., Roy, A., Grandidier, J.C., 2013. A study of the impact of humid aging on the strength of industrial adhesive joints. Int. J. Adhesion Adhesives 44, 66–77.
Leprince, J.G., Palin, W.M., Hadis, M.A., Devaux, I., Leloup, G., 2013. Progress in dimethacrylatebased dental composite technology and curing efficiency. Dent. Mater. 29 (2), 139–156.
Li, C., Strachan, A., 2011. Molecular dynamics predictions of thermal and mechanical properties of thermoset polymer EPON862/DETDA. Polymer 52 (13), 2920–2928.
Li, J., Li, H., Fok, A. S.L., Watts, D.C., 2009a. Multiple correlations of material parameters of light-cured dental composites. Dent. Mater. 25 (7), 829–836.
Li, L., Yu, Y., Wu, Q., Zhan, G., Li, S., 2009b. Effect of chemical structure on the water sorption of amine-cured epoxy resins. Corros. Sci. 51 (12), 3000–3006.
Lien, W., Vandewalle, K.S., 2010. Physical properties of a new silorane-based restorative system. Dent. Mater. 26 (4), 337–344.
Loshaek, S., 1955. Crosslinked polymers.-II. Glass temperatures of copolymers of methyl methacrylate and glycol dimethacrylates. J. Polym. Sci. 15 (80), 391–404.
Lu, X., Jiang, B., 1991. Glass transition temperature and molecular parameters of polymer. Polymer 32 (3), 471–478.
Mainjot, A.K., Dupont, N.M., Oudkerk, J.C., Dewael, T.Y., Sadoun, M.J., 2016. From artisanal to CAD-CAM blocks: state of the art of indirect composites. J. Dent. Res. 95 (5), 487–495.
Malacarne-Zanon, J., Pashley, D.H., Agee, K.A., Foulger, S., Corrêa Alves, M., Breschi, L., et al., 2009. Effects of ethanol addition on the water sorption/solubility and percent conversion of comonomers in model dental adhesives. Dent. Mater. 25 (10), 1275–1284.

Mante, F.K., Wadenya, R.O., Bienstock, D.A., Mendelsohn, J., LaFleur, E.E., 2010. Effect of liquid rubber additions on physical properties of Bis-GMA based dental resins. Dent. Mater. 26 (2), 164–168.

Mark, J.E., 1984. The rubber elastic state (Chapter 1) In: Mark, J.E., Eisenberg, A., Graessley, W.W., Mandelkern, L., Koenig, J.L. (Eds.), Physical Properties of Polymers. American Chemical Society, Washington, DC, pp. 1–54.

Masouras, K., Silikas, N., Watts, D.C., 2008. Correlation of filler content and elastic properties of resin-composites. Dent. Mater. 24 (7), 932–939.

Mayo, F.R., Lewis, F.M., 1944. Copolymerization. I. A basis for comparing the behavior of monomers in copolymerization; the copolymerization of styrene and methyl methacrylate (Review). J. Am. Chem. Soc. 66 (9), 1594–1601.

Merdas, I., Thominette, F., Tcharkhtchi, A., Verdu, J., 2002. Factors governing water absorption by composite matrices. Compos. Sci. Technol. 62 (4), 487–492.

Miyazaki, T., Hotta, Y., Kunii, J., Kuriyama, S., Tamaki, Y., 2009. A review of dental CAD/CAM: current status and future perspectives from 20 years of experience. Dent. Mater. J. 28 (1), 44–56.

Morel, E., Bellenger, V., Verdu, J., 1985. Structure-water absorption relationships for amine-cured epoxy resins. Polymer 26 (11), 1719–1724.

Moszner, N., Salz, U., 2001. New developments of polymeric dental composites. Prog. Polym. Sci. 36, 535–576.

Mott, P.H., Dorgan, J.R., Roland, C.M., 2008. The bulk modulus and Poisson's ratio of "incompressible" materials. J. Sound Vibration 312 (4–5), 572–575.

Moy, P., Allan Gunnarsson, C., Weerasooriya, T., Chen, W., 2011. Stress-strain response of PMMA as a function of strain-rate and temperature. In: "Dynamic Behavior of Materials, Volume 1". Proceedings of the 2011 Annual Conference on Experimental and Applied Mechanics, pp. 125–133.

Munhoz, T., Fredholm, Y., Rivory, P., Balvay, S., Hartmann, D., da Silva, P., et al., 2017. Effect of nanoclay addition on physical, chemical, optical and biological properties of experimental dental resin composites. Dent. Mater. 33 (3), 271–279.

Murli, C., Song, Y., 2010. Pressure-induced polymerization of acrylic acid: a Raman spectroscopic study. J. Phys. Chem. B 114 (30), 9744–9750.

Musanje, L., Darvell, B.W., 2006. Curing-light attenuation in filled–resin restorative materials. Dent. Mater. 22 (9), 804–817.

Musanje, L., Ferracane, J.L., Sakaguchi, R.L., 2009. Determination of the optimal photoinitiator concentration in dental composites based on essential material properties. Dent. Mater. 25, 994–1000.

Nakabayashi, N., Nakamura, M., Yasuda, N., 1991. Hybrid layer as a dentin-bonding mechanism. J. Esthetic Dent. 3 (4), 133–138.

Narayanaswamy, O.S., 1971. A model of structural relaxation in glass. J. Am. Ceram. Soc. 54 (10), 491–498.

Nguyen, J.F., Migonney, V., Ruse, N.D., Sadoun, M., 2012. Resin composite blocks via high-pressure high-temperature polymerization. Dent. Mater. 28 (5), 529–534.

Nguyen, J.F., Migonney, V., Ruse, N.D., Sadoun, M., 2013. Properties of experimental urethane dimethacrylate-based dental resin composite blocks obtained via thermopolymerization under high pressure. Dent. Mater. 29 (5), 535–541.

Omran Alhareb, A., Md Akil, H., Arifin Ahmad, Z., 2017. Impact strength, fracture toughness and hardness improvement of PMMA denture base through addition of nitrile rubber/ceramic fillers. Saudi J. Dent. Res. 8 (1–2), 26–34.

Ornaghi, B.P., Meier, M.M., Lohbauer, U., Braga, R.R., 2014. Fracture toughness and cyclic fatigue resistance of resin composites with different filler size distributions. Dent. Mater. 30 (7), 742–751.
O'Brien, W.J., 2008. Dental Materials and Their Selection, fourth ed. Quintessence Publishing Company.
Pal, R., 2005. New models for effective Young's modulus of particulate composites. Composites: Part B 36, 513–523.
Papadogiannis, D., Tolidis, K., Gerasimou, P., Lakes, R., Papadogiannis, Y., 2015. Viscoelastic properties, creep behavior and degree of conversion of bulk fill composite resins. Dent. Mater. 31 (12), 1533–1541.
Papakonstantinou, A.E., Eliades, T., Cellesi, F., Watts, D.C., Silikas, N., 2013. Evaluation of UDMA's potential as a substitute for Bis-GMA in orthodontic adhesives. Dent. Mater. 29 (8), 898–905.
Paris, P.C., Gomez, M.P., Anderson, W.P., 1961. A rational analytic theory of fatigue. Trend Eng. 13, 528–534.
Park, J.-G., Ye, Q., Topp, E.M., Misra, A., Spencer, P., 2009. Water sorption and dynamic mechanical properties of dentin adhesives with a urethane-based multifunctional methacrylate monomer. Dent. Mater. 25 (12), 1569–1575.
Park, J.W., Ferracane, J.L., 2006. Residual stress in composites with the thin-ring-slitting approach. J. Dent. Res. 85 (10), 945–949.
Pascault, J.P., Williams, R.J.J., 1990. Relationships between glass transition temperature and conversion. Polym. Bull. 24 (1), 115–121.
Pascault, J.-P., Sauterau, H., Verdu, J., Williams, R.J.J., 2002a. Thermosetting polymers (Chapter 7). Are Cured Thermosets Inhomogeneous? Taylor & Francis.
Pascault, J.-P., Sautereau, H., Verdu, J., Williams, R.J.J., 2002b. Thermosetting Polymers. Marcel Dekker, Inc (Chapter 11).
Pérez, J., Cavaille, J.Y., Diaz Calleja, R., Gómez Ribelles, J.L., Monleón Pradas, M., Ribes Greus, A., 1991. Physical ageing of amorphous polymers. Theoretical analysis and experiments on poly(methyl methacrylate). Macromol. Chem. Phys. 192 (9), 2141–2161.
Pethrick, R.A., Davis, W.J., 1998. Towards a molecular approach to physical ageing in poly(methyl methacrylate). Polym. Int. 47 (1), 65–71.
Phan, A.C., Tang, M.-L., Nguyen, J.-F., Ruse, N.D., Sadoun, M., 2014. High-temperature high-pressure polymerized urethane dimethacrylate—mechanical properties and monomer release. Dent. Mater. 30 (3), 350–356.
Powers, J.M., Sakagushi, R.L., 2006. Craig's Restorative Dental Materials, twelfth ed. Elsevier, Saint-Louis, MO.
Rahim, T.N., Mohamad, D., Md Akil, H., Ab Rahma, I., 2012. Water sorption characteristics of restorative dental composites immersed in acidic drinks. Dent. Mater. 28 (6), e63–e70.
Ramsteiner, F., Armbrust, T., 2001. Fatigue crack growth in polymers. Polym. Test. 20 (3), 321–327.
Raskin, A., 2011. Les résines composites. Société Francophone de Biomatériaux Dentaires [© Université Médicale Virtuelle Francophone].
Raskin, A., Salomon, J.P., Tassery, H., Sabbagh, J., 2006. Les résines composites propriétés et indications cliniques. Réalités cliniques 16, 313–326.
Richaud, E., Gilormini, P., Coquillat, M., Verdu, J., 2014. Crosslink density changes during the hydrolysis of tridimensional polyesters. Macromol. Theory Simul. 23 (5), 320–330.
Roberts, D.E., 1950. Heat of polymerization. A summary of published values and their relation to structure. J. Res. Natl. Bureau Standards. 44, 221–232.

Rüttermann, S., Dluzhevskaya, I., Großsteinbeck, C., Raab, W.H.-M., Janda, R., 2010. Impact of replacing Bis-GMA and TEGDMA by other commercially available monomers on the properties of resin-based composites. Dent. Mater. 26 (4), 353–359.
Sakagushi, R.L., Powers, J.M., 2012. Craig's Restorative Dental Materials, thirteenth ed. Elsevier Mosby.
Schettino, V., Bini, R., Ceppatelli, M., Citroni, M., 2008. Activation and control of chemical reactions at very high pressure. Phys. Scripta 78, Article 058104.
Schnabel, W., 1978. In: Jellinek, H.H.G. (Ed.), Aspects of Polymer Degradation and Stabilization. Elsevier, Oxford and New York, pp. 149–190.
Semen, J., Lando, J.B., 1969. The acid hydrolysis of isotactic and syndiotactic poly(methyl methacrylate). Macromolecules 2 (6), 570–575.
Shah, M.B., Ferracane, J.L., Kruzic, J.J., 2009. Mechanistic aspects of fatigue crack growth behavior in resin based dental restorative composites. Dent. Mater. 25, 909–916.
Shen, C.H., Springer, G.S., 1976. Moisture absorption and desorption of composite materials. J. Compos. Mater. 10 (1), 2–20.
Shortall, A.C., Wilson, H.J., Harrington, E., 1995. Depth of cure of radiation-activated composite restoratives – influence of shade and opacity. J. Oral Rehabil. 22 (5), 337–342.
Sideridou, I.D., Karabela, M.M., 2011. Sorption of water, ethanol or ethanol/water solutions by light-cured dental dimethacrylate resins. Dent. Mater. 27 (10), 1003–1010.
Sideridou, I., Tserki, V., Papanastasiou, G., 2002. Effect of chemical structure on degree of conversion in light-cured dimethacrylate-based dental resins. Biomaterials 23 (8), 1819–1829.
Sideridou, I., Tserki, V., Papanastasiou, G., 2003. Study of water sorption, solubility and modulus of elasticity of light-cured dimethacrylate-based dental resins. Biomaterials 24 (4), 655–665.
Sideridou, I., Achilias, D.S., Spyroudi, C., Karabela, M., 2004. Water sorption characteristics of light-cured dental resins and composites based on Bis-EMA/PCDMA. Biomaterials 25 (2), 367–376.
Sideridou, I.D., Karabela, M.M., Vouvoudi, E.C., 2008. Volumetric dimensional changes of dental light-cured dimethacrylate resins after sorption of water or ethanol. Dent. Mater. 24 (8), 1131–1136.
Siu-Wai Kong, E., 1986. Physical Aging in Epoxy Matrices and Composites. Advances in Polymer Science 80. Springer-Verlag Berlin Heidelberg, pp. 125–171.
Skibo, M.D., Hertzberg, R.W., Manson, J.A., Kim, S.L., 1977. On the generality of discontinuous fatigue crack growth in glassy polymers. J. Mater. Sci. 12 (3), 531–542.
Smith, L.S.A., Schmitz, V., 1988. The effect of water on the glass transition temperature of poly(methyl methacrylate). Polymer 29 (10), 1871–1878.
Soderholm, K.J., Mariotti, A., 1999. BIS-GMA--based resins in dentistry: are they safe? J. Am. Dent. Assoc. 130 (2), 201–209.
Soles, C.L., Chang, F.T., Gidley, D.W., Yee, A.F., 2000. Contributions of the nanovoid structure to the kinetics moisture transport in epoxy resins. J. Polym. Sci. Part B: Polym. Phys. 38, 776–791.
Stansbury, J.W., 2012. Dimethacrylate network formation and polymer property evolution as determined by the selection of monomers and curing conditions. Dent. Mater. 28 (1), 13–22.
Struik, L.C.E., 1978. Physical Aging in Amorphous Polymers and Other Materials. Elsevier, Amsterdam, pp. 61–65 (Chapter 6).

ten Brinke, G., Karasz, F.E., Ellis, T.S., 1983. Depression of glass transition temperatures of polymer networks by diluents. Macromolecules 16 (2), 244–249.
Thomaidis, S., Kakaboura, A., Mueller, W.D., Zinelis, S., 2013. Mechanical properties of contemporary composite resins and their interrelations. Dent. Mater. 29 (8), e132–e141.
Thominette, F., Pabiot, J., Verdu, J., 1989. Effect of radiolysis on the glass transition temperature of poly (methyl methacrylate). Makromol. Chem. Macromol. Symp. 21 (1), 255–267.
Thonemann, B., Schmalz, G., Hiller, K.A., Schweikl, H., 2002. Responses of L929 mouse fibroblasts, primary and immortalized bovine dental papilla-derived cell lines to dental resin components. Dent. Mater. 18 (4), 318–323.
Tillman, M.S., Hayes, B.S., Seferis, J.C., 2002. Examination of interphase thermal property variance in glass fiber composites. Thermochim. Acta 392–393, 299–302.
Van Krevelen, D.W., Te Nijenhuis, K., 2009. Chap 6. Properties of Polymers – Their Correlation with Chemical Structure; Their Numerical Estimation and Prediction from Additive Group Contributions, fourth, completely revised ed. Elsevier, Amsterdam.
Van Landuyt, K.L., Yoshihara, K., Geebelen, B., Peumans, M., Godderis, L., Hoet, P., et al., 2012. Should we be concerned about composite (nano-)dust? Dent. Mater. 28 (11), 1162–1170.
Van Noort, R., 2012. The future of dental devices is digital. Dent. Mater. 28 (1), 3–12.
Vieth, W.R., Howell, J.M., Hsieh, J.H., 1976. Dual sorption theory. J. Memb. Sci. 1, 177–220.
Wada, H., 1992. Determination of dynamic fracture toughness for PMMA. Eng. Fract. Mech. 41 (6), 821–831.
Watanabe, H., Khera, S.C., Vargas, M.A., Qian, F., 2008. Fracture toughness comparison of six resin composites. Dent. Mater. 24 (3), 418–425.
Wei, Y.-J., Silikas, N., Zhang, Z.-T., Watts, D.C., 2011. Diffusion and concurrent solubility of self-adhering and new resin–matrix composites during water sorption/desorption cycles. Dent. Mater. 27 (2), 197–205.
Xu, H.H., Smith, D.T., Jahanmir, S., Romberg, E., Kelly, J.R., Thompson, V.P., et al., 1998. Indentation damage and mechanical properties of human enamel and dentin. J. Dent. Res. 77 (3), 472–480.
Zimm, B.H., Lundberg, J.L., 1956. Sorption of vapors by high polymers. J. Phys. Chem. 60 (4), 425–428.